Journal of Computational Design and Engineering 6 (2019) 296–315

Contents lists available at ScienceDirect

Journal of Computational Design and Engineering

journal homepage: www.elsevier.com/locate/jcde

Optimum design of hydraulic water retaining structures incorporating uncertainty in estimating heterogeneous hydraulic conductivity utilizing stochastic ensemble surrogate models within a multi-objective multi-realisation optimisation model

Muqdad Al-Juboori [a,b,*], Bithin Datta [c]

[a] College of Science and Engineering, James Cook University, Townsville, QLD 4811, Australia
[b] College of Engineering, Wasit University, Wasit, Iraq
[c] Discipline of Civil Engineering, College of Science and Engineering, James Cook University, Townsville, QLD 4811, Australia

ARTICLE INFO

Article history:
Received 10 June 2018
Received in revised form 11 December 2018
Accepted 22 December 2018
Available online 24 December 2018

Keywords:
Reliability based optimum design
Heterogeneous hydraulic conductivity
Non-dominated sorting genetic algorithm
Hydraulic water retaining structure
Multi-objective multi-realisation optimisation model
Numerical seepage analysis

ABSTRACT

In order to find optimum and reliable designs for hydraulic water retaining structures (HWRSs), a reliability based optimum design (RBOD) model was used to quantify uncertainty in estimates of seepage characteristics due to uncertainty in heterogeneous hydraulic conductivity (HHC). This included incorporating reliability measures into minimum-cost HWRS designs and utilising a multi-realisation optimisation technique based on various stochastic ensemble surrogate models. To improve the efficiency of the RBOD model and the direct search optimisation solver, a multi-objective multi-realisation optimisation (MOMRO) model was employed. Some of the stochastic optimisation constraints could be formulated as a second objective function to be minimised in the MOMRO model. This can significantly improve the search efficiency of the multi-objective non-dominated sorting genetic algorithm-II (NSGA-II) that was used, and help determine more feasible candidate solutions in the search space. Gaussian process regression was used to develop the surrogate models, which were trained on numerous datasets created from numerical seepage simulations. The effect of uncertainty was also considered for other HWRS safety factors and conditions, such as overturning, flotation, sliding and eccentric loading. The results demonstrate that uncertainty in HHC estimates significantly impacts optimum HWRS design. Therefore, deterministic optimum solutions that are created based on expected values of hydraulic conductivity are not adequate for reliable HWRS design. The developed MOMRO model, which was based on an ensemble approach, addresses some of the uncertainty in HHC values that affects HWRS design. Also, the MOMRO technique improves the efficiency of the optimisation search process and facilitates a direct search process to provide many optimum alternatives.

1. Introduction

The application of geotechnical engineering processes involves a wide range of uncertainties due to soil properties variation. The primary sources of uncertainty are long-term environmental effects, errors in laboratory measurements and statistical analyses, and inadequate numbers of samples with which to characterise the soil. As a result, it is difficult to determine the behaviour of each element in the underground soil environment. Uncertainty in soil parameters substantially affects design variables and, thus, can have adverse consequences on the safety of a structure. Therefore, the reliability of a design is an essential consideration in engineering designs and applications. Reliability analysis requires analysis of the soil parameters statistical characteristics, design criteria and the methods that determine the reliability of the design. Accordingly, the reliability based optimum design (RBOD) model was employed in this study to quantify the reliability component of the design process while managing uncertainties in estimates of soil seepage characteristics due to uncertainties in the

Peer review under responsibility of Society for Computational Design and Engineering.

* Corresponding author.
E-mail addresses: muqdad.aljuboori@my.jcu.edu.au (M. Al-Juboori), bithin.datta@jcu.edu.au (B. Datta).
URLs: http://orcid.org/0000-0001-9148-8563, https://scholar.google.com.au/citations?user=8cr3nxQAAAAJ&hl=en (M. Al-Juboori), http://scholar.google.com.au/citations?user=uwHmi3sAAAAJ&hl=en, https://www.researchgate.net/profile/Bithin_Datta/publications (B. Datta).

https://doi.org/10.1016/j.jcde.2018.12.003
2288-4300/

Nomenclature and Abbreviations

RBOD	reliability based optimum design
HHC	heterogeneous hydraulic conductivity
HC	hydraulic conductivity (m/day)
HWRS	hydraulic water retaining structure
FEM	finite element method
MOMRO	multi-objective multi-realisation optimisation
d_1	upstream cut-off depth (m)
d_2	downstream cut-off depth (m)
b	width of HWRS (m)
b^*	part of floor on the upstream side of HWRS
H	upstream water head (m)
HS	Halton sequences
LHS	Latin hypercube sampling method
Pc_1	uplift pressure on upstream (m)
Pe_2	uplift pressure on downstream (m)
ie	exit gradient
μ	mean
σ	standard deviation
CV	coefficient of variation

estimation of heterogeneous hydraulic conductivity (HHC). Furthermore, the RBOD model employed was formulated based on the multi-objective multi-realisation optimisation (MOMRO) technique, which utilises various surrogate models in order to determine the optimum design of a hydraulic water retaining structure (HWRS).

An HWRS design is significantly influenced by the quantity of seepage. Also, large spatial and directional variations in hydraulic conductivity (HC), which has a large coefficients of variation (CV) in the order of 200–300% (Baecher & Christian, 2005), will affect HWRS seepage analyses and determination of seepage quantities such as exit gradient and uplift pressure. Homogenous or isotopic soils are rarely found in the field (Freeze, 1975; Lambe & Whitman, 2008). Recently, geotechnical and structural design codes have strongly recommended the incorporation of uncertainty in analyses of the properties of materials, parameters, loads, analytical methods and experimental error, in order to address design uncertainty (ACI Committee American Concrete Institute & International Organisation for Standardization, 2011; Standardization, 2004). Therefore, the parameter of heterogeneous hydraulic conductivity (HHC) was considered in the present study. Values of HHC were randomly drawn from log-normal distributions based on different CV values. Incorporating HHC in seepage analysis related to HWRS design in this way provides a basis for safe and quantifiably reliable design.

Seepage analysis must be accurate and applicable to complex flow domains involving HHC. Even for homogenous, simple and symmetrical flow domains, closed-form seepage analysis under HWRS is a complex exercise involving conformal mapping transformation and complex integrals (Harr, 2012). Accordingly, many imprecise approximation theories and methods applicable to simple cases have been developed for simplified seepage analysis under HWRS (Bligh, 1915; Khosla, Bose, & Taylor, 1936; Lane, 1935). However, all these methods and theories are inapplicable to complex flow domains in porous media. However, numerical seepage simulation based on the finite element method (FEM) could be used to accurately determine seepage quantities such as HHC in complex flow domains (Cho, 2012; Griffiths & Fenton, 1993; Shahrbanozadeh, Barani, & Shojaee, 2015).

The effects of uncertainty and variation in soil properties on design reliability have been studied extensively (Baroni, Zink, Kumar, Samaniego, & Attinger, 2017; Christian, Ladd, & Baecher, 1994; Deng, Li, Qi, Cao, & Phoon, 2017; Duncan, 2000; Hicks & Spencer, 2010; Hicks, Nuttall, & Chen, 2014; Popescu, Deodatis, & Nobahar, 2005). Specifically, for seepage related to hydraulic structures, most studies have concentrated on the stochastic analysis of seepage characteristics based on different realisations of hydraulic conductivity generated from different probability distribution functions (PDF) or different sets of means and standard deviations (Ahmed, 2012; Griffiths & Fenton, 1993, 1997; Le, Gallipoli, Sanchez, & Wheeler, 2012). The most significant conclusion of these studies is that seepage characteristics are significantly influenced by the degree of uncertainty in parameter estimates. Consequently, this may negatively affect the performance and safety of designs. Recently, some studies have utilised stochastic simulations in designs, which incorporated a random field with a numerical simulation to quantify the designs' reliability. For example, Griffiths and Fenton (2004) used a random FEM, and Zhu, Wang, Li, Liu, and Cheng (2017) utilised a weighted dynamic response surface method. A non-intrusive stochastic finite element method was used by Jiang, Li, Zhang, and Zhou (2014), and a multi-response surface method was utilized by Deng et al. (2017). Other researchers have replaced computationally-expensive numerical simulations with stochastic response surface models to quantify reliability (Mollon, Dias, & Soubra, 2009, 2010). Due to the complexities involved in reliability analysis, uncertainty in estimates of soil parameters and its consequences for optimisation models have received little attention in previous geotechnical and hydraulic structure studies.

Incorporating reliability into HWRS design promotes understanding of its consequences and also provides safer designs. Minimising construction costs is an important goal in large engineering constructions such as HWRSs, and more conservative designs can be inefficient in terms of cost. In addition, as massive amounts of construction material and engineering effort are required for such projects, cost-efficient HWRS designs can significantly reduce total construction costs. Hence, in this study, a RBOD technique based on the MOMRO framework was utilised to determine optimal HWRS designs that provide the desired reliability at the minimum cost.

Since a numerical model was used to analyse seepage quantities incorporating different realisations of HHC, it was difficult to utilise conventional reliability analysis methods (Baecher & Christian, 2005). As a result, the reliability method utilised in this study was based on a multi-realisation concept based on multiple stochastic responses of a numerical seepage simulation. Since directly linking a simulation model to a RBOD model is a time-consuming and computationally-expensive task, especially with problems incorporating HHC, many ensemble surrogate models were developed and linked to the RBOD model to accurately predict the stochastic responses of seepage characteristics for HWRSs.

The objective of this study was to determine reliable and cost-effective optimised HWRS designs that incorporate uncertainty in estimates of HHC. The methodology implemented was based on a RBOD framework that uses the MOMRO technique, which integrates multiple stochastic responses from well-trained surrogate models based on Gaussian process regression (GPR) machine learning techniques. These stochastic responses represent the uncertainties in estimates of particular seepage design variables that are embedded in the stochastic constraints and objective functions

of MOMRO. The reliability criterion is quantified by imposing reliability constraints. The final optimum design must satisfy the constraints, which are based on a specified fraction of the ensemble of predictive surrogate models that satisfy the designated reliability constraints. Further, the estimated reliability is based on the ratio of the number of individual surrogate models satisfying the reliability constraints of the design criteria to the total number of models in the ensemble. Or, a number of satisfactions can be imposed that are equivalent to the stochastic constraints to reflect the imposed reliability of the design criteria. Stochastic constraints which imposed on an HWRS design to satisfy a safe exit gradient value were formulated as a second stochastic objective function. The optimization solver, the non-dominated sorting genetic algorithm-II (NSGA-II), minimised two stochastic objectives: the exit gradient and construction cost. The desired reliability levels were implicitly incorporated in the objective functions and explicitly incorporated in the constraints. The simulation model used and the formulation of the optimal design are discussed in the following sections.

2. Material and methods

2.1. Seepage conceptual model and design of experiments

In an HWRS, the seepage process is governed by the Laplace equation. The Laplace equation for seepage analysis shown in Eq. (1) is restricted to homogeneous isotopic hydraulic conductivity and assumed steady-state conditions. Otherwise, it is difficult to find a close form solution for HWRS seepage characteristics for HHC.

$$k_x \frac{\partial^2 h}{\partial x^2} + k_y \frac{\partial^2 h}{\partial y^2} + k_z \frac{\partial^2 h}{\partial z^2} = 0 \quad (1)$$

where k_x, k_y and $k_z$are the hydraulic conductivity coefficients in the *x*, *y* and *z* directions, respectively, and h is the hydraulic head. Alternatively, a numerical technique based on FEM can be used to solve the Laplace equation for HHC problems and determine the seepage characteristics. However, the numerical model does not provide a generalised and explicit relationship for seepage analysis that can be incorporated in the RBOD model.

Direct linkage of the numerical seepage modelling (FEM) code to the RBOD model is not possible. The model geometry and numerical model boundary conditions are varied for each new candidate decision vector through the optimisation process. The FEM mesh number, properties and location are also varied. Furthermore, directly linking the numerical model to the RBOD model is a time-consuming task, as NSGA-II invokes the numerical model numerous times to evaluate the objective functions and constraints for all candidate solutions presented by the optimisation solver. Besides, numerical seepage simulation for cases including HHC takes more time than simulations of cases encompassing homogenous hydraulic conductivity. For example, the simulation time of a case with an HHC drawn from a log-normal distribution (CV = 182.5%) was 2.37 min. The simulation used in the present study was implemented on a relatively high-speed processor (Intel® Core™ i7-2600 64x-based processor running at 3.4 GHz with 8.00 GB RAM). Assuming that it is technically possible to link the simulation model to optimisation model (S-O), and using a population size of 1000 and 100 generations with the NSGA-II-based RBOD, the optimisation algorithm requires 100,000 iterations to evaluate the constraints and objective functions and reach the optimum solution. Subsequently, one optimisation run requires 3950 h (based on 2.37 min for each iteration), which is inefficient. The directly linking S-O models has been conducted previously by other researchers and similar conclusions have been reached (Dhar & Datta, 2009; Mollon, Dias, & Soubra, 2009, 2010).

Hence, indirect linkage of the S-O model was adopted in this study by linking it with trained surrogate models in order to accurately imitate numerically obtained seepage responses. The first step to developing the surrogate model was to propose a conceptual model for seepage analysis under HWRS. This model included design variables related to seepage analysis. The input design variables represented the upstream and downstream cut-off depths (d_1, d_2), the width of the HWRS (b), and the upstream water head (H). The downstream side was the seepage potential face with a zero water level, as shown in Fig. 1. The input design variables of the conceptual models for each case were numerically processed to determine output data (seepage characteristics) for the same case. Several sets of input data could be generated and numerically simulated to obtain input-output data sets with which to train the surrogate models.

The input data set was randomly generated using the Halton sequences (HS) method (Loyola, Pedergnana, & García, 2016). The HS method can provide a more uniform distribution of generated data and is better than the Latin hypercube sampling (LHS) method. The HS method can uniformly cover the entire space of the variable limits, whereas the LHS method leaves some regions without any points, and many points may be found in the same location, as shown in Fig. 2. In developing a robust surrogate model, having uniform input data provides more information and experience with which to enhance the machine learning process.

The ranges for the input design variables were d_2, d_1 = 0–80 m and b, H = 0–150 m. These limits were proposed to cover the high percentage of expected dimensions of a newly constructed HWRS. The number of generated data for use as input design variables was 150 random cases. However, because a random field HHC was used, the number of simulations for each of the input design variables was 20, including 20 different realisations of HHC for each case to cover a wide range of uncertainty in HHC. Each single realisation represented a unique and randomly varied distribution of the hydraulic conductivity values of the finite elements used in the numerical model. Five log-normal distributions with different standard deviations (σ = 0.85, 1.55, 2.25, 2.95, 3.65) and a constant

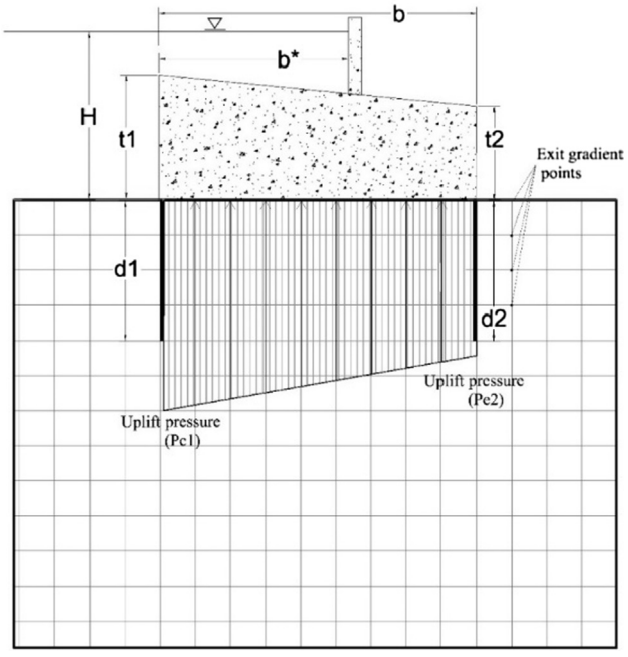

Fig. 1. The conceptual model of a HWRS.

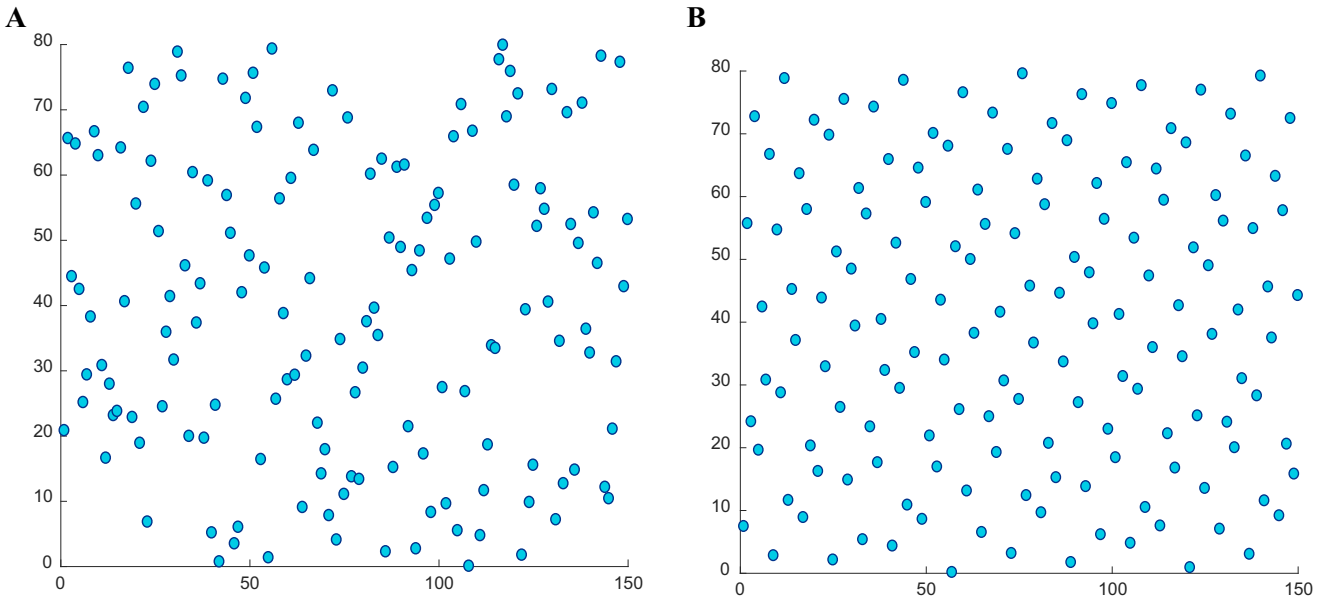

Fig. 2. Random data sampling using (A) LHS method. (B) HS method for the width of HWRS [d_1 (0–80) m].

mean ($\mu = 2$) were proposed to generate different CV values (42.5, 77.5, 112.5, 147.5, 182.5%) of HHC. Therefore, four realisations were randomly generated utilising a specified log-normal distribution. These generated values were used in the numerical seepage simulation for each case of the input design variables (d_1, d_2, b, H). The Geo-Studio/SEEPW numerical code (Krahn, 2012) was used to simulate each case separately. As a result, each input dataset was simulated 20 times to generate different (stochastic) output datasets reflecting the uncertainty of seepage characteristics due to random variation in HHC.

The output datasets encompassed uplift pressure on the upstream and downstream sides (Pc_1, Pe_2), and exit gradient values at four locations (ie_1, ie_2, ie_3, ie_4), as shown in Fig. 1. The exit gradient values were considered for four points to provide greater safety to the HWRS for such a heterogeneous flow domain. Consequently, for each input design variable set (d_1, d_2, b, H), there were 20 different output seepage characteristic sets (Pc_1, Pe_2, ie_1, ie_2, ie_3, ie_4) associated with 20 different HHC realisations. Additionally, for each output design seepage variable, 20 surrogate models were trained and tested to imitate the stochastic numerical responses. A stochastic ensemble surrogate model was developed for each set of seepage quantities and contained the 20 surrogate models. Therefore, for a single input dataset, 20 stochastic responses were obtained by the ensemble surrogate model for processing in the MOMRO models.

The Box-Muller approximation method (Ross, 2014) was utilised to generate an uncorrelated random field drawn from a log-normal distribution (μ, σ). A sub-code was written in C# then linked to the Geo-studio/SEEPW seepage modelling code. This code provided a random value for each finite element in the numerical model, and a totally new realisation of the random field was presented by this code for each run. Examples of different realisations of random fields for a single characteristic of the log-normal distribution are presented in Figs. 3-A1 and 3-A2. Furthermore, the effect of these realisations on the exit gradient and uplift pressure distributions are presented in Figs. 3-B1, 3-B2, 3-C1 and 3-C2. These figures demonstrate that there is significant variation in seepage quantities due to the different realisations of HHC. Hence, there were noticeable uncertainties associated with the seepage quantities.

2.2. Design and evaluation of the surrogate models

Designing and developing an efficient surrogate model requires considerable effort and a systematic procedure. It may be simpler and faster to train a surrogate model and achieve precise training performance, but this does not ensure that the surrogate model remains accurate when used to test datasets containing values beyond the training data ranges. Therefore, the surrogate model design process must include a robust machine learning technique, good learning experience obtained by well-distributed training data sets, and sensitive measures of error to evaluate the training and testing performance of the surrogate models developed.

The Gaussian process regression (GPR) machine learning technique was employed to develop the surrogate models utilised in the current study. The GPR technique can efficiently provide an accurate prediction for the training and testing phases (Rasmussen, 2004). GPR is relatively unaffected by noisy training data and its generalisability is better than that of other machine learning techniques such as support vector machines and artificial neural networks (He et al., 2017; Kang, Han, Salgado, & Li, 2015; Kang, Xu, Li, & Zhao, 2017; Li et al., 2017; Pal & Deswal, 2010; Samui & Jagan, 2013).

Briefly, the GPR technique can explore numerous relationships between input and output datasets based on random vectors following the Gaussian distribution. The GPR technique can identify the best relationship based on the concept that the unknown function would accurately describe this relationship if the output of any proposed random vector is close to the target datasets (Rasmussen, 2004; Roberts et al., 2013). The GPR technique drives a function $f(x)$ to describe the relationship based on the mean function ($m(x)$) and the covariance function$k(x, x_*)$ of the random vector, where x_* is the observed data. The GPR function is similar to the multivariate Gaussian distribution, as shown in Eq. (2).

$$f(x)\ \mathcal{GP}(m(x), k(x, x_*)), \mathrm{x} \ni \mathbb{R} \tag{2}$$

The developed GPR surrogate models were trained using the Matlab programming language. The parameters of GPR listed in Table 1 were selected after many trial-and-error iterations to achieve the best prediction with minimum error in the training and testing phases. Furthermore, different scenarios of training/

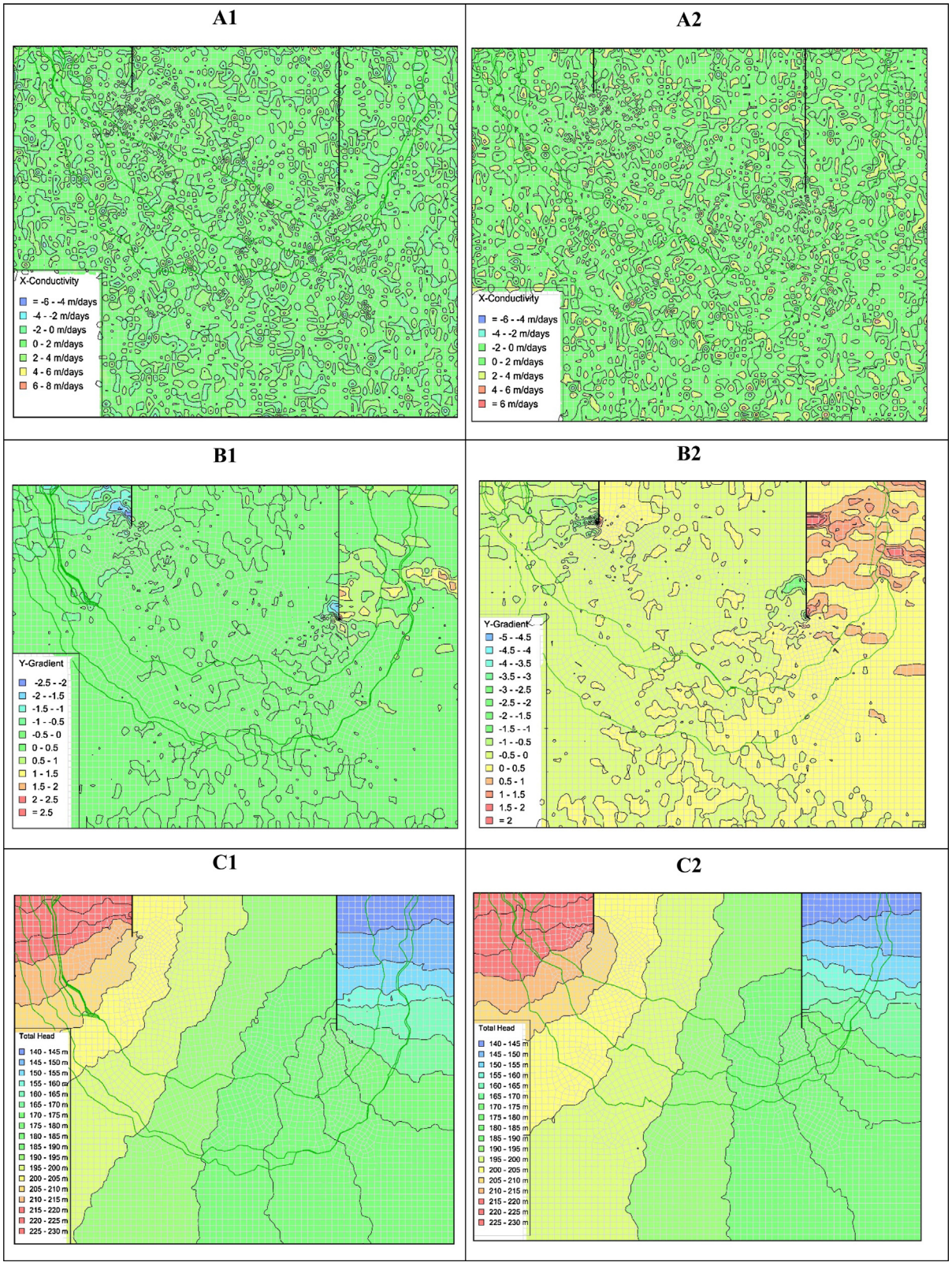

Fig. 3. A randomly selected case, including different realization of HHC (A_1, A_2) drawn from a same standard deviation (2, 3.65). B_1, B_2 effect the different realization of HHC (A_1, A_2) on the exit gradient distribution. C_1, C_2 effect the different Realization of HHC (A_1, A_2) on the total head distribution.

testing data were randomly selected and tested to find the best set of GPR parameters for each surrogate model. The other parameters were left the same as the default Matlab values.

The source data was divided into training and testing data sets. Since it is recommended that the majority of the data be used for training (Alpaydin, 2014) and because the testing set does not

Table 1
Parameters of the GPR technique.

Properties	value
Prediction method	exact
Kernel function	Squared exponential kernel with a separate length scale per predictor
Fit method	Exact
Basis function	Constant

affect the performance of the surrogate models, 90% of the source data was used for training and 10% was used for testing. The generalisability of the GPR surrogate models was examined by evaluating the predictive accuracy of the surrogate models outside the training dataset. The testing error should be close to the training error and both must be within the prescribed ranges. However, because the source data was obtained from stochastic numerical simulations, the training and testing results were slightly less robust, especially for cases with a high CV random field.

Before using them in an RBOD model, the training/testing performance of surrogate models must be accurately evaluated. The developed GPR surrogate models were strictly evaluated using many error measures and statistical evaluation indices. Descriptions and equations for each measure are summarised in Table 2 and more detail can be found in Gupta, Sorooshian, and Yapo (1999) and Moriasi et al. (2007).

Where $\hat{y}$ is the predicted data, y is the observed data, and $\bar{y}$ and $\bar{\hat{y}}$ refer to the means of the observed and predicted data, respectively. These error measures were applied to all surrogate models. The majority of surrogate models presented perfect training and testing performance. Although the testing prediction efficiency of some models was suboptimal, their predictions were still within the accepted ranges, particularly the exit gradient surrogate models of cases with high uncertainty (CV = 182.5%, 147.5%). Samples of the training and testing results of the developed surrogate models are presented in Table 3 and Figs. 4–9. The letters (A, B, C and D) in the Table and Figures below refer to the four different realizations of source data used to training the surrogate models, e.g. A refers to the first realization and B refers to the second realization, etc. These results reflect the training of the GPR technique with noisy training datasets influenced by uncertainty in HHC.

2.3. Multi-objective multi-realisation optimisation model

Formulation of a multi-realisation optimisation model based on a single objective function with numerous stochastic constraints may lead to a sub-optimum or infeasible solution due to the large number of constraints that must be imposed as binding conditions for the optimum solution. In this study, many attempts were made to formulate an RBOD model with large numbers of stochastic constraints and a single objective function; however, the solutions obtained were infeasible. Several previous studies have compared the performance of multi-objective and single objective optimisation models (Yapo, Gupta, & Sorooshian, 1998; Zakaria, Jamaluddin, Ahmad, & Loghmanian, 2012). These studies concluded that multi-objective formulations may provide more efficient solutions than those obtained by single-objective models. Such conclusions seem to have been based on the premise that if a large number of constraints are replaced by a suitable objective function (second objective function), which does not need achieving a specified level as constraints need, the computation becomes more flexible and, possibly, more efficient. Further, since multi-realisation technique-based reliability computation requires a large number of stochastic constraints, an optimisation search process based on evolutionary algorithms may produce infeasible solutions. This is due to the fact that searching efficiency decreases with increases in the number of constraints and the complexity of the problem (Dorsey & Mayer, 1995; Kolda, Lewis, & Torczon, 2003). Furthermore, incorporating a large number of stochastic constraints makes it difficult to determine the direction in which to improve the search process, because the stochastic constraints for each iteration provide different responses reflecting the uncertainties in the design parameters and variables.

Therefore, a new formulation for the RBOD model was adopted in this study in order to improve the search process for such complex optimisation tasks. The most important stochastic constraints are the exit gradient constraints, as they are significantly influenced by HHC uncertainty and have critical impacts on the design

Table 2
Descriptions of utilized error measures.

Measure name	Functionality	Range	Accepted range	Equation
Correlation coefficient (R)	Evaluate the linear relationship between observed and predicted data	−1 to +1	≥0.5	$R=\frac{\sum_{i=1}^{n}(\hat{y}_i-\bar{\hat{y}})(y_i-\bar{y})}{\sqrt{\sum_{i=1}^{n}(\hat{y}_i-\bar{\hat{y}})^2(y_i-\bar{y})^2}}$
Nash- Sutcliffe efficiency (NSE)	Measures the residual variance to the measured data variance	−∞ to +1	0 and 1	$NSE=1-\left[\frac{\sum_{i=1}^{n}(\hat{y}_i-y_i)^2}{\sum_{i=1}^{n}(y_i-\bar{y})^2}\right]$
Percent bias (PBIAS)	Provide a perspective about how much the average of the Predicted data is larger or smaller than their counterpart observed data	Positive values refer that the model overestimation, and negative values refer that the model is underestimation	ideal value is 0	$PBIAS=\frac{\sum_{i=1}^{n}(y_i-\hat{y}_i)\times 100}{\sum_{i=1}^{n}(y_i)}$
RMSE to standard deviation ratio (RSR)	Provides an indication of the error ratio to the standard deviation of the observed data	≥0	ideal value is 0	$RSR=\frac{RMSE}{STD_{obs}}=\frac{\sqrt{\sum_{i=1}^{n}(y_i-\hat{y}_i)^2}}{\sqrt{\sum_{i=1}^{n}(y_i-\bar{y})^2}}$

Table 3
Samples of the surrogate models training/testing error measures.

	ie1 (2.95-B)		ie2(1.55-C)		ie3(1.55-D)		ie4 (2.95-A)		pc1(3.65-C)		pe2(3.65-B)	
	train	test	train	test	train	test	train	test	train	test	train	test
MSE	0.00	0.03	0.02	0.05	0.05	0.07	0.07	0.06	20.52	12.08	4.16	24.73
STD-ERROR	0.00	0.19	0.14	0.22	0.22	0.27	0.27	0.24	4.55	3.52	2.05	4.95
M-error	0.00	0.01	0.00	0.03	0.00	0.06	0.00	0.02	0.00	−0.73	0.00	−1.35
NSE	1.00	0.71	0.93	0.67	0.81	0.74	0.81	0.70	0.97	0.99	0.99	0.98
RSR	0.00	0.54	0.26	0.57	0.43	0.51	0.44	0.55	0.16	0.11	0.08	0.16
PBIAS	0.00	3.66	0.00	5.51	0.00	11.11	0.00	5.32	0.00	−1.64	0.00	−3.24
R	0.99	0.88	0.96	0.82	0.90	0.87	0.91	0.84	0.98	0.99	0.99	0.99

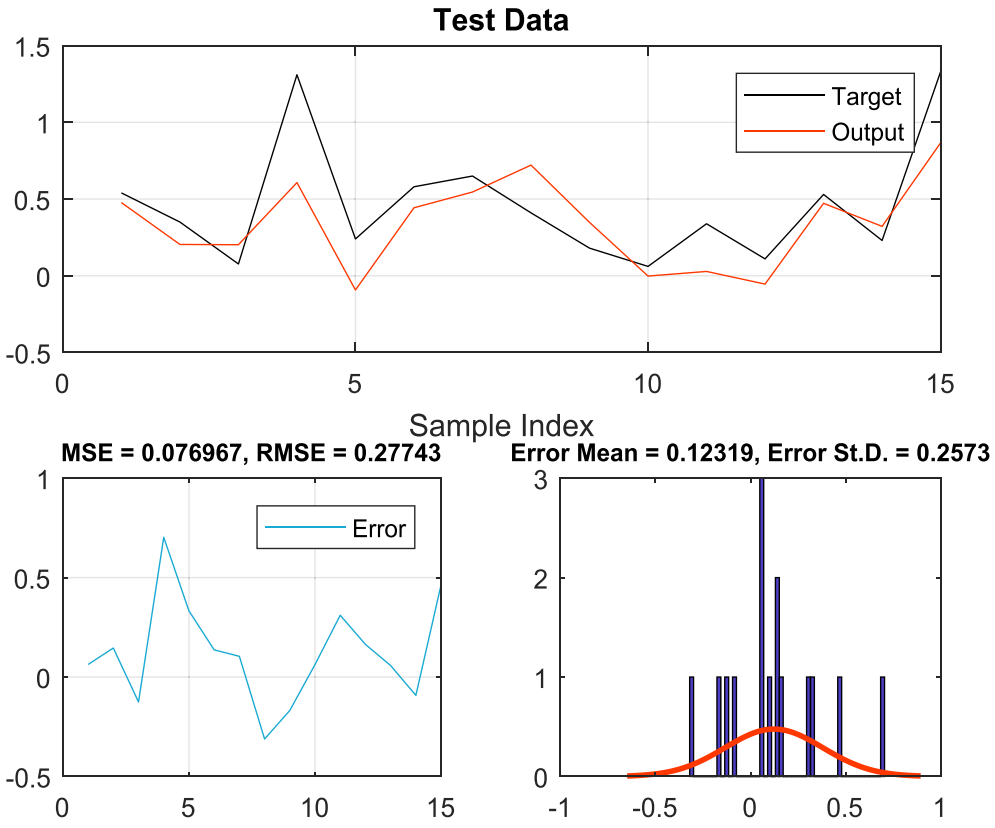

Fig. 4. The ie_4 surrogate model prediction for test data (σ = 2.95-D).

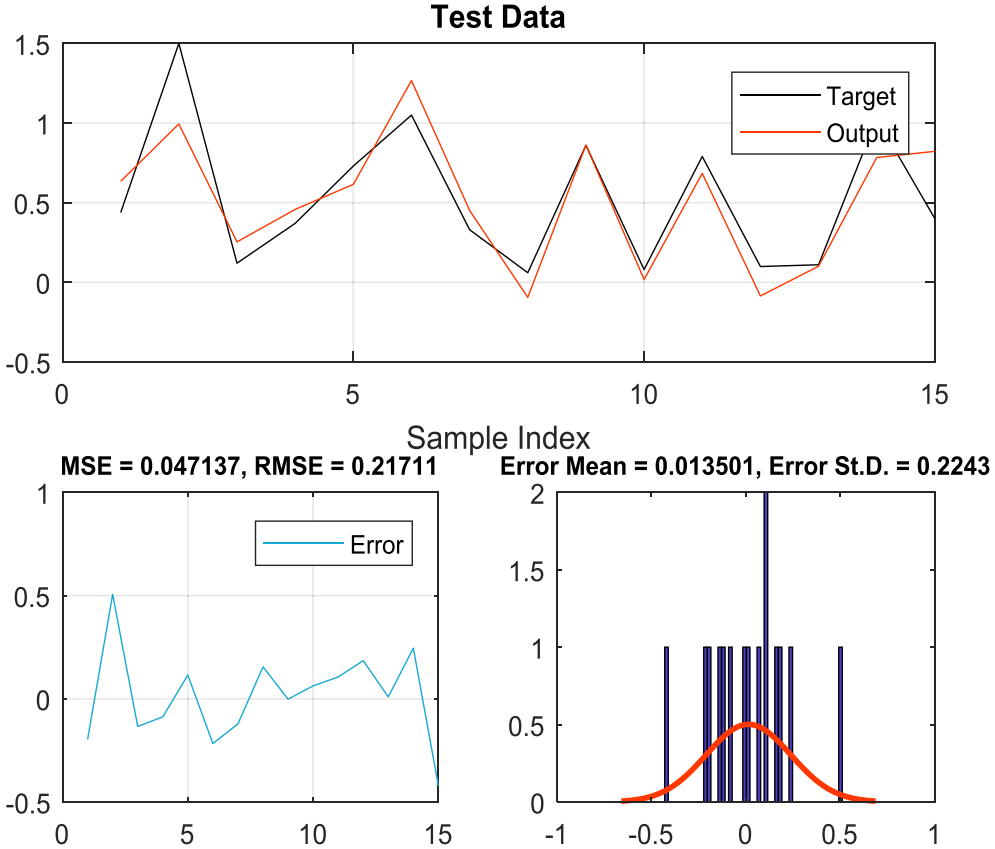

Fig. 5. The pc1 surrogate model prediction for test data (σ = 3.65-D).

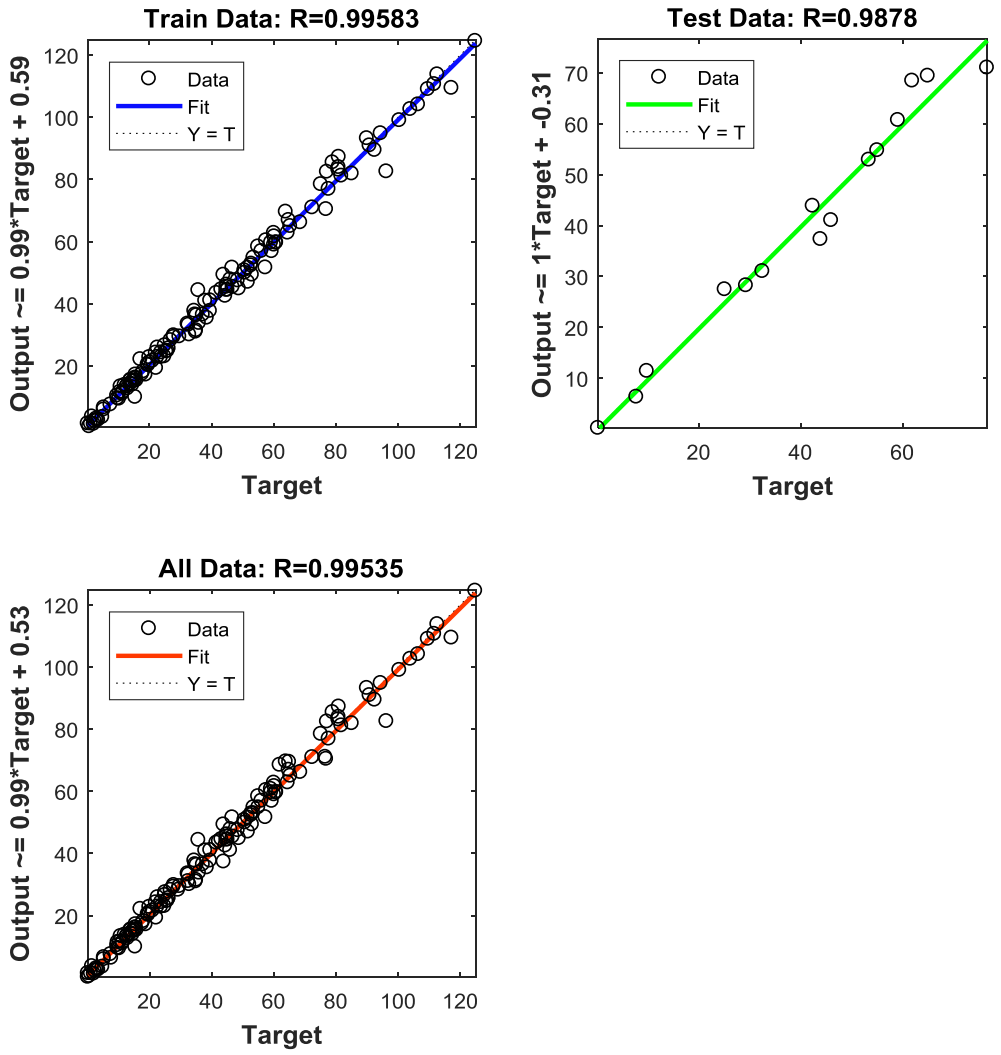

Fig. 6. Training- testing R index for the surrogate model (ie_4) ($\sigma = 2.25$-C).

and safety of HWRSs (Al-Juboori & Datta, 2018a). These constraints were transformed into a second objective function to be minimised in addition to the HWRS construction cost objective function. Hence, the multi-objective optimisation formulation was implemented to significantly decrease the number of constraints and improve the searching efficiency. The reliability was also included for the exit gradient objective function and implemented for the minimum cost objective functions and other stochastic constraints using the multi-realisation technique (Section 2.5).

The optimum solution of the multi-objective optimisation model is not a single solution; therefore, a set of optimum solutions is presented. Each consecutive solution represents an improvement in the first objective and deterioration in the second objective function. Hence, there is no solution explicitly better than the others, and designers have many alternatives from which to select the optimum design for their HWRS.

2.4. Non-dominated Sorting Genetic Algorithm-II (NSGA-II)

In many engineering applications, two or more conflicting objectives are possible. Improving one objective may lead to the sacrifice of other conflicting objectives. Hence, it is inappropriate to present a single solution to a multi-objective optimisation model. Instead, a set of non-dominated optimum solutions (Pareto optimum solutions) are generated. Multi-objective formulation does not result in an optimum solution for each objective function separately, as it does in a single objective function. There are many in-between solutions in which the optimal performance of the design can be identified (Burke & Kendall, 2005).

The process of utilising NSGA-II to attain the Pareto optimal front and the process of obtaining a non-dominated set of solutions to finally select an optimal solution are briefly described here. The non-dominated optimum solution X dominates the solution Y if X is not worse than Y in all the objective function values, and X is better than Y in one objective. The NSGA-II is a population-based search algorithm that is similar to a genetic algorithm (GA) (Gen & Cheng, 2000).

NSGA-II starts with N random initial populations, P_0. Thereafter, ordinary GA operations, such as binary tournament selection, crossover and mutation operations, are performed to generate an offspring population Q_t of size N. The individuals in P_0 and Q_t are combined to generate $2N$ populations and the best non-dominated sorting individuals are used to fill different ranks of Pareto fronts (slots), one by one. The highest-ranked non-dominated front is obtained first, then the second one, etc. Since there are $2N$ individuals and all non-dominated fronts could not cover more than N individuals, all exceeded individuals are rejected (Zakaria et al., 2012). The selection process for filling the last slot is slightly different because it probably has two parts and all the individuals in that slot have the same rank. The population of the first part

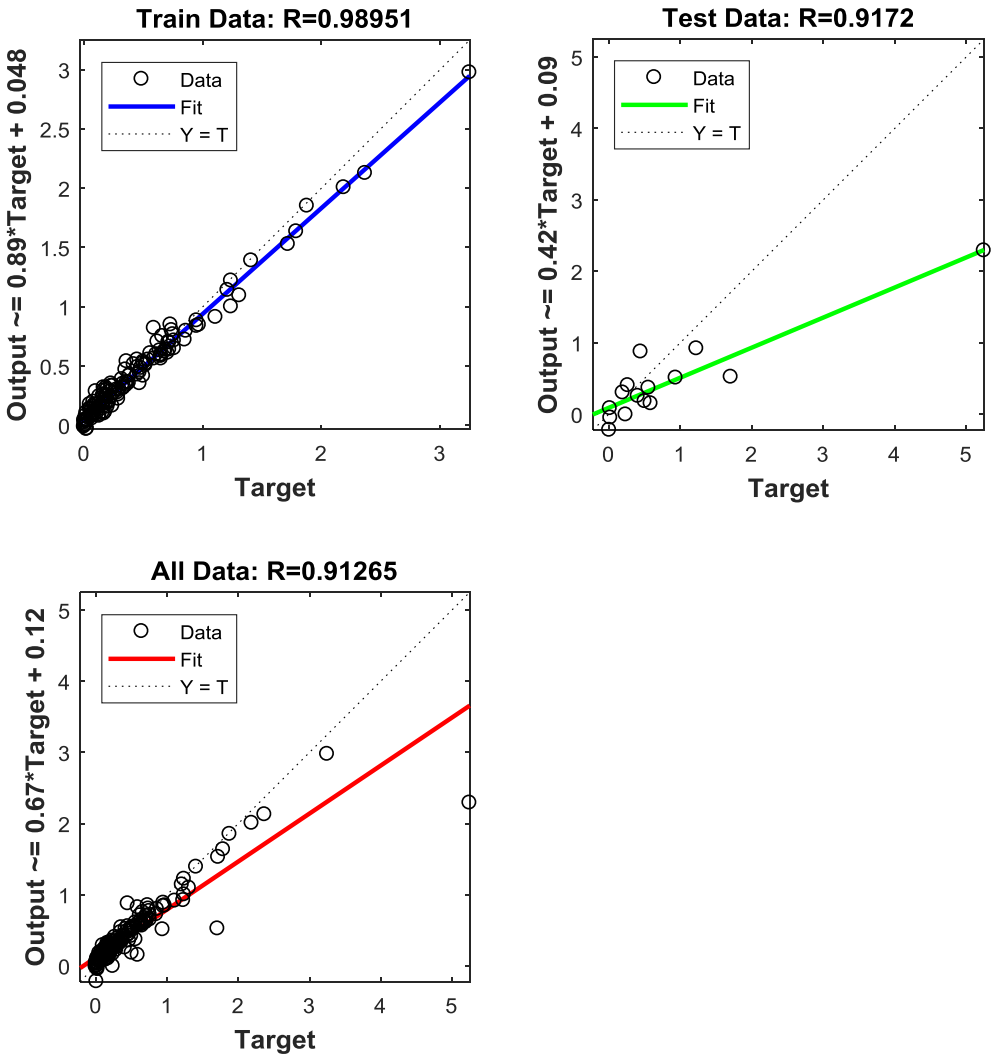

Fig. 7. Training- testing R index for the surrogate model (ie_2) (σ = 3.65-B).

would be within *N*, and the second part of the population would be more than *N*, which must be deleted, as described in Fig. 10. Instead of using an unsystematic process to fill the last slot, the crowding distance measure is used to select more diverse individuals.

The crowding distance is a second preference metric after non-dominated ranking. If two solutions are selected from the same Pareto front, then the solution resulting from the less crowded area (larger crowding distance d_i) is the winner. Determining the crowding distance for a solution **i** is based on the two neighbouring solutions located in either side of **i** for the Pareto front. The distance d_i represents the average cuboid sides determined, based on the location of the nearest solutions (i + 1, i − 1), as shown in Fig. 11 (Burke & Kendall, 2005). The crowding distance (d_i^m) for solution **i** for each objective function (f^m,m = 1, 2, …, M) is given by Eq. (3). Many researchers have utilised NSGA-II in finding the optimum solution trade-off for competing objective functions, inferring that the performance was efficient (Bekele & Nicklow, 2007; Deb, 2001; Rajabi-Bahaabadi, Shariat-Mohaymany, Babaei, & Ahn, 2015; Yandamuri, Srinivasan, & Murty Bhallamudi, 2006).

$$d_i^m = d_i^m + \frac{f_{i+1}^m - f_{i-1}^m}{f_{max}^m - f_{min}^m} \tag{3}$$

The parameters of the utilized optimisation solver (NSGA-II) are listed in Table 4. These parameters were selected based on repeated attempts to find the best combinations. The rest of the parameters were left as the default Matlab options. As the ranges of the two objective functions are significantly different, and the option of the allowable tolerance for the objective functions was applied for all the objective functions, the exit gradient objective function value was magnified by a scale factor of 1000 to provide a smoother evaluation for both objectives.

2.5. Formulation the reliability based MOMRO model

The multi-realisation optimisation technique is based on formulation of the stochastic constraints utilising the predictions of developed ensemble stochastic surrogate models. For each safety factor or condition in the HWRS optimisation model, there is a single ensemble stochastic surrogate model encompassing 20 surrogate models' responses for a specified seepage design variable. The desired reliability level is attained by allowing the optimum solution to satisfy any fraction (n) out of the total number (m = 20) of constraints for a certain stochastic constraint. The required reliability level is equivalent to n/m. The multi-realisation optimisation technique reflects uncertainty in

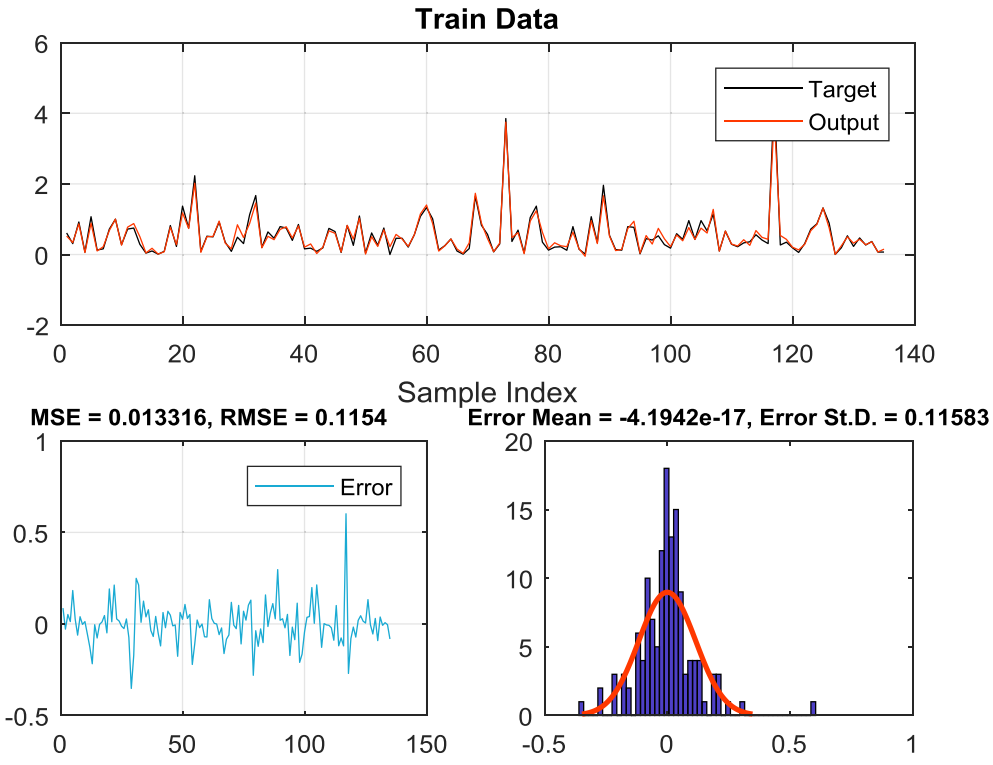

Fig. 8. The ie_2 surrogate model training performance ($\sigma = 2.95$-A).

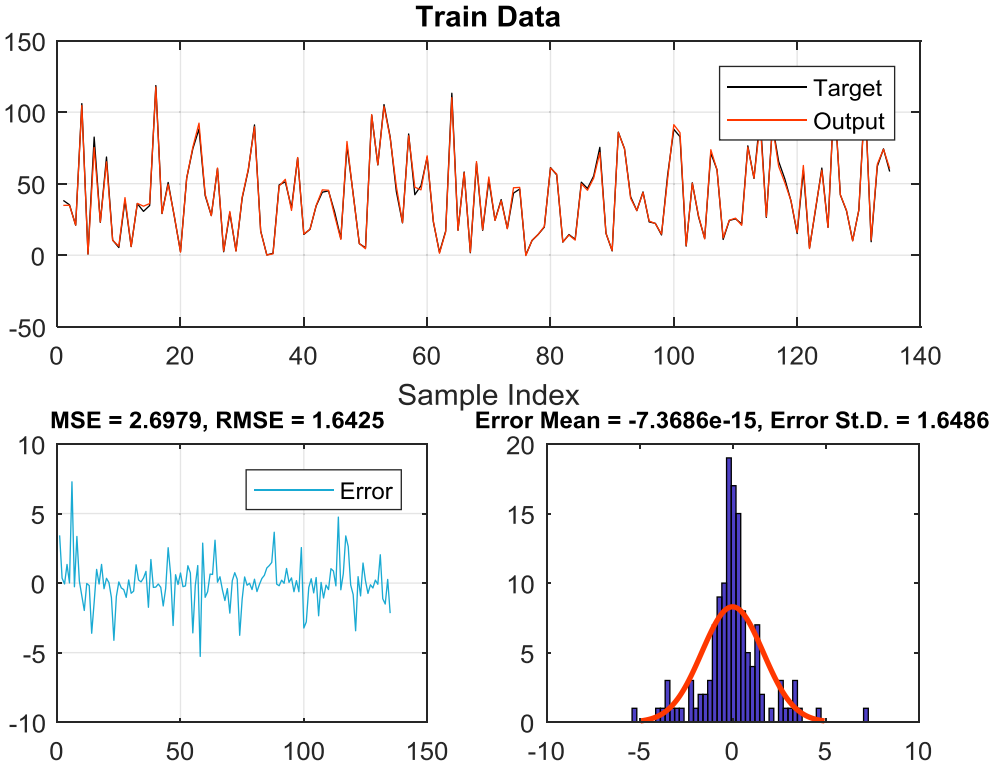

Fig. 9. The pc1 surrogate model training performance ($\sigma = 2.95$-D).

the seepage quantities due to the uncertainty of the HHC. For instance, 80% reliability means that the optimum solution satisfies 16 (any) of the 20 stochastic constraints related to each design safety factor of HWRS.

A multi-realisation technique based the reliability measure was also incorporated in the objective functions in the MOMRO model. The second objective function, which minimised the exit gradient value, integrated the reliability measure by incorporating the exit

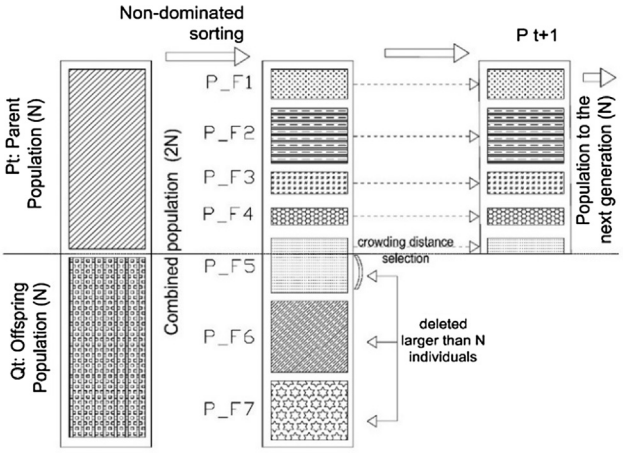

Fig. 10. Non-dominated sorting and Pareto front selection process (NSGA-II).

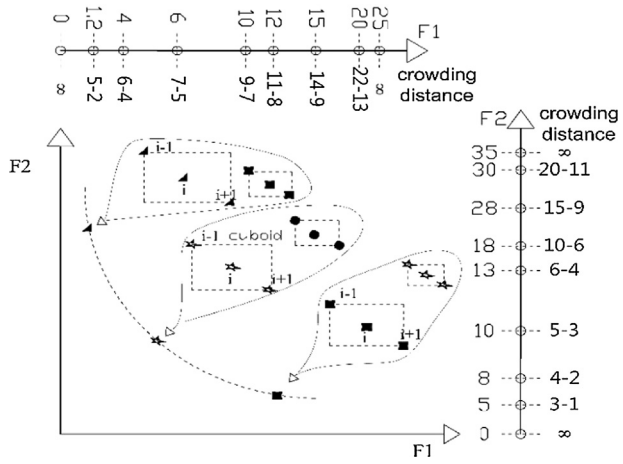

Fig. 11. Crowding distance selection process to fill the last Pareto.

Table 4
Utilized NSGA-II parameters for the MOMRO model.

Options	Value
Population size	1000
Crossover fraction	0.6
Pareto fraction	0.45
Max generations	200
Function tolerance	1e-3
Constraint tolerance	1e-3
Crossover function	Crossover intermediate
Migration direction	Both

gradient stochastic responses in the determination of the objective function. Since the exit gradient objective function was minimised, the 20 stochastic exit gradient responses based on the ensemble stochastic surrogate models were determined and sorted in ascending order. The maximum value of all the obtained exit gradient values was selected to be minimised. This is equivalent to 99.9% reliability, because the resulting exit gradient value is the safest estimate, as all other stochastic values are less than the obtained exit gradient. To attain 80% reliability, for example, we impose the optimisation solver to minimise the fifth maximum value (based on 20 responses) and allow up to four stochastic responses of exit gradient to be higher than the one chosen for the objective function value.

Since there are four locations to determine the exit gradient value (ie_1, ie_2, ie_3, ie_4), the maximum value (based on a specified reliability level) for each location was determined, and the average of these values was considered in the second objective function. The same technique was applied to determine the first objective function that of minimising the HWRS construction cost. The construction cost is based on the upstream and downstream floor thicknesses (t_1, t_2), and the depths of the upstream and downstream cut-offs (d_1, d_2), plus the width (b) of HWRS, as shown in Fig. 1. These Variables are based on the stochastic responses of the seepage characteristics ensemble surrogate models.

Furthermore, the proposed constraints shown in Eqs. (7)–(15) represent the design requirements and safety factors that must be satisfied by the resulting optimum solution for a safe design. These conditions and safety factors are sliding, overturning and flotation safety factors, plus eccentric load conditions. Similarly, such safety factors have been considered as deterministic constraints in linked S-O models to obtain optimum HWRS designs for different scenarios (Al-Juboori & Datta, 2017a, 2017b, 2018a, 2018b). However, in the current study, these constraints are stochastic constraints, and the exit gradient stochastic constraints are integrated as a second objective function (Eq. (5)).

The formulation of the optimisation model for MOMRO is as shown below:

$$\text{Find} X = \{x_1, x_2, x_3, x_4,\} = \{d_1, d_2, b, b^*\}$$

$$\text{Minimise}: f_1(X) = c_f b \frac{\max_{(m-\omega)}(t_1^m) + \max_{(m-\omega)}(t_2^m)}{2} + t_c \sum_{s=1}^{2} c_s^c d_s \quad (4)$$

$$\text{Minimise}: f_2(X) = \frac{\max_{(m-\omega)}(ie_1^m) + \max_{(m-\omega)}(ie_2^m) + \max_{(m-\omega)}(ie_3^m) + \max_{(m-\omega)}(ie_4^m)}{4} \quad (5)$$

$$ie_i^m = \varepsilon_i^m(H, d_1, d_2, b, k_m) \forall i, m \quad (6)$$

Subject to:

$$Fs_{fl-us}^m \geq 1.3 \forall m$$

$$Fs_{fl-us}^m = \epsilon^m(H, d_1, d_2, b, k_m) \forall m \quad (7)$$

$$Fs_{fl-ds}^m \geq 1.3 \forall m$$

$$Fs_{fl-ds}^m = \gamma^m(H, d_1, d_2, b, k_m) \forall m \quad (8)$$

$$Ecc^m \geq \frac{b}{3} \forall m$$

$$Ecc^m \leq \frac{2b}{3} \forall m$$

$$Ecc^m = \frac{Mpas^m - Mact^m}{Vload^m} \forall m \quad (9)$$

$$Fs_{over}^m \geq 1.5 \forall m$$

$$Fs_{over}^m = \frac{Mpas^m}{Mact^m} \forall m \quad (10)$$

$$Fs_{slid}^m \geq 1.5 \forall m$$

$$Fs_{slid}^m = \frac{C \times b + f \times Vl^m}{Hl} \forall m \quad (11)$$

$$Mpas^m = f^m(H, b, b^*, t_1^m, t_2^m, k_m, G_c, G_w, pc_1^m, pe_2^m)\forall m \quad (12)$$

$$Mact^m = f^m(H, b, b^*, t_1^m, t_2^m, k_m, G_c, G_w, pc_1^m, pe_2^m)\forall m \quad (13)$$

$$Vl^m = f^m(H, b, b^*, t_1^m, t_2^m, k_m, G_c, G_w, pc_1^m, pe_2^m)\forall m \quad (14)$$

$$Hl = f(H, G_w) \quad (15)$$

$$k_m = Lognormal(\mu, \sigma)\forall m, k_m \in (0, \infty)$$

and the reliability constraints:

$$Z_{q\_logical}^m = Fs_q^m \geq or \leq Fs_{qallowable}^m \forall q, m$$

$$g(x)_q = \sum^m Z_{logical}^m \leqslant DR\forall q \quad (16)$$

where $max_{(m-\omega)}$ is a function sorting the stochastic responses in ascending order, and returns the $(m-\omega)^{\text{th}}$ value of the sorted vector. m is the number of stochastic responses (20), ω is based on the desired reliability level; e.g., when $\omega = 0$, the reliability is 99.9% and when $\omega = 4$, the reliability is 80%, etc. t_1^m and t_2^mrepresent the stochastic thickness values of the floor at the upstream and downstream sides, respectively. c_f is the construction cost of the floor per cubic meter ($400/m^3), c_c is the construction cost of the cut-offs per cubic meter, which is a function of the depth of the cut-off (d_1, d_2) as shown in Eq. (17), and t_c is the thickness of the sheet pile, which equals 1.0 m.

$$c_s^c = d_s^3 + 20d_s^2 + 200d_s + 400\forall s \quad (17)$$

ie_i^m is the **m** realisations of the exit gradient safety factor determined based on **m** surrogate models $\{\varepsilon_i^m()\}$, and for each location (i) there are **m** realisations of the exit gradient safety factor. Fs_{fl-us}^m, FFs_{fl-ds}^m are stochastic safety factors imposing the weight of the upstream and downstream floors of the HWRS to safely counterbalance the uplift pressures ($Pc_1{}^m$,$Pe_2{}^m$) (Bligh, 1915; U.S. Army Corps of Engineers, 1987).

Computation of Fs_{fl-us}^m and FFs_{fl-ds}^m is mainly based on the developed stochastic surrogate models $Pc_1{}^m\{\epsilon^m()\}$and $Pe_2{}^m$ $\{\gamma^m()\}$, respectively. Ecc^m is a design condition to prevent the eccentric load condition on the foundation of the HWRS. $Mpas^m$ is the passive momentum obtained from all the forces increasing the stability of the HWRS, $Mact^m$ is the active momentum obtained from the all forces decreasing the stability of the HWRS, $Vload^m$is the result of the all vertical loads influencing on the HWRS. $Mpas^m, Mact^m, Vload^m$are functions to $(H, b, b^*, t_1^m, t_2^m, k_m, G_c, G_w, pc_1^m, pe_2^m)$, as shown in Eqs. (12)–(14). Fs_{over}^m is the overturning stochastic safety factor, and Fs_{slid}^m is the stochastic sliding safety factor. C = cohesion resistance soil properties, and f =tan ∅, where ∅ is the internal friction angle (Lj, 2014). The values of f and C are assumed to be f =tan ∅ = 0.7 and C = 20 kPa. Hl is the resultant of all the horizontal loads affecting the HWRS.

Variable k_m represents different realisations of the HHC based on different CV values and implicitly affects the prediction of the stochastic seepage quantity. $Z_{q\_logical}^m$ is a logical variable used to check the violation of the constraints associated with a **q** number of safety factors for m stochastic realisations. DR is the reliability of all the constraints and objective functions needed to satisfy a certain reliability level in the HWRS design.

Additionally, there are many other logical and boundary constraints utilised to prevent the optimisation solver from presenting illogical and negative values. A flowchart of the reliability based MOMRO model is shown in Fig. 12.

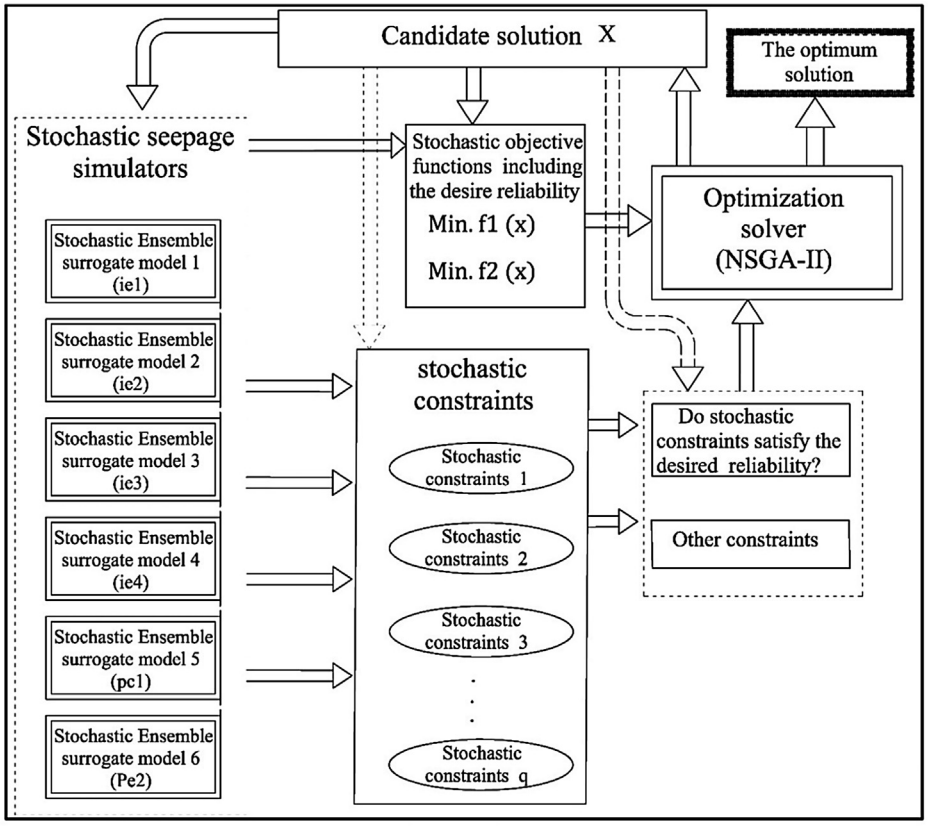

Fig. 12. Schematic representation of the reliability based MOMRO stochastic S-O model.

2.6. Computing efficiency

Computational efficiency is a crucial factor in achieving an expeditious RBOD model. The optimum solution is based on various assumed design and parameter scenarios. Therefore, these solutions require the development of different sets of surrogate models for performance evaluation purposes. In real life design problems, multiple scenarios are not taken into design consideration and evaluation. Therefore, in this evaluation-based study, a number of surrogate models for different scenarios of design assumptions and parameter values were required to be trained. The number of surrogate models needed to be limited to reduce the enormous computational time that would otherwise be required in such an evaluation process. In addition, incorporation of the surrogate models as approximate simulation models within the linked S-O model actually makes it feasible for a simulation model to be solved numerous times within a linked S-O model. Therefore, computational efficiency can also be viewed from a feasibility point of view.

Moreover, formulation of a reliability based MOMRO model is computationally-expensive and time-consuming, even when surrogate models are used instead of numerical simulation models. In each iteration of the S-O model, the optimisation solver needs to invoke the 120 responses of the developed surrogate model twice to evaluate the stochastic objective functions and the constraints. Furthermore, NSGA-II uses a large number of evaluations of a large number of random populations to attain the global optimum solution. Hence, solving such optimisation problems using traditional techniques consumes too much time. One roughly selected optimisation run was implemented using the traditional computing technique based on 1000 populations. The time required for the run was 14,100 s (≈ 4 h). The traditional computing technique was based on writing the constraint and objective functions codes in two separate files. Each file calls the 120 developed surrogate models for each iteration. For each iteration of the S-O mode, the outcomes of the objective functions and constraints codes are passed to the optimisation solver after 240 responses are attained, based on 120 trained surrogate models. This procedure is inefficient, as many optimisation runs need to be completed.

Alternatively, to increase computing efficiency, a nested function technique was utilised (MathWorks, 2015). By using the nested function, both the constraint and objective function codes could be written in the same file. The stochastic surrogate models were uploaded one at a time, and the resulting objective functions and constraint values computed by the nested function were simultaneously returned as a vector to the optimisation solver. NSGA-II was formulated to adapt the nested function output. This strategy doubled the computational speed.

More importantly, in evolutionary optimisation algorithms utilising the random population search technique, the evaluation process for the objective functions and constraints are based on having one individual in each iteration, and this process continues until all candidate individuals are evaluated. Then, the same procedure is implemented for the second generation, etc. This process takes a longer time compared to the vector-process, which could substantially speed up the optimisation process. By utilising the vector-process, all individuals are evaluated at once to determine the stochastic constraints and objective functions. The evaluation outcome for each iteration is a matrix whose length is equal to the population size. Each column vector represents a certain value of the optimisation variables, such as the constraints or the objective function values versus the individuals. The optimisation solver evaluates the improvement direction for each element in the vector. That means the whole population is evaluated at once, and then the improvement direction is determined by selecting the high-ranking individuals in the matrix. This process continues to the next new generation until the stopping criteria are satisfied.

Implementing the vector-process combined with the nested function for the reliability based MOMRO model resulted in an efficient processing time of around 500 s. Although formulating optimisation codes based on the vector-process takes some time and effort, it was computationally efficient. This strategy provided greater flexibility with which to make repeated systematic trial iterations and find the best parameter combinations that provided the best performance in NSGA-II.

3. Results and discussion

The reliability based MOMRO model was applied to hypothetical design cases. These cases included five upstream head values (100 m, 80 m, 60 m, 40 m, 20 m), each of which was implemented at four reliability levels (99.9%, 80%, 60%, 40%). The reliability level was explicitly integrated in the stochastic constraints and implicitly in the objective functions. The competed objective functions were the minimum exit gradient and minimum construction cost of the HWRS.

The obtained Pareto optimum fronts for each head value and reliability level are presented in Figs. 13–17. Each Pareto front includes a wide range of optimum solutions for each head value associated with each reliability level. To make an appropriate

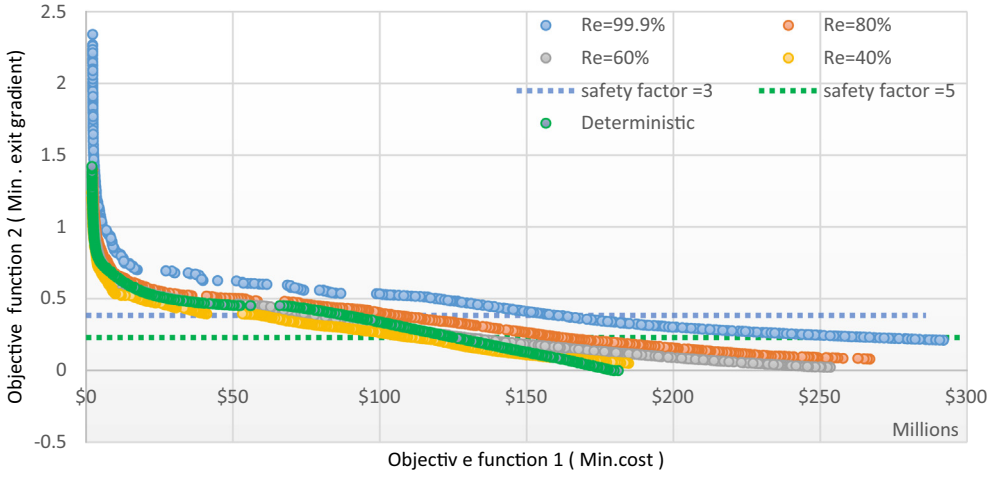

Fig. 13. Pareto front for different reliability levels (H = 100).

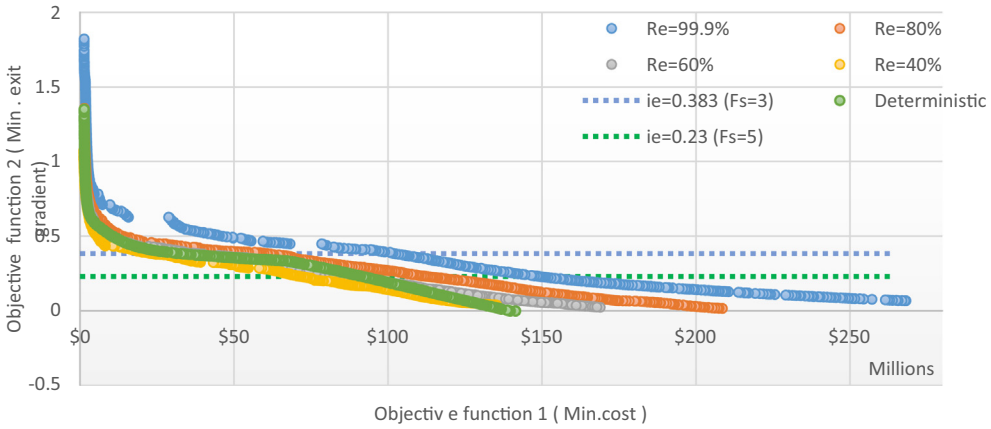

Fig. 14. Pareto front for different reliability levels (H = 80).

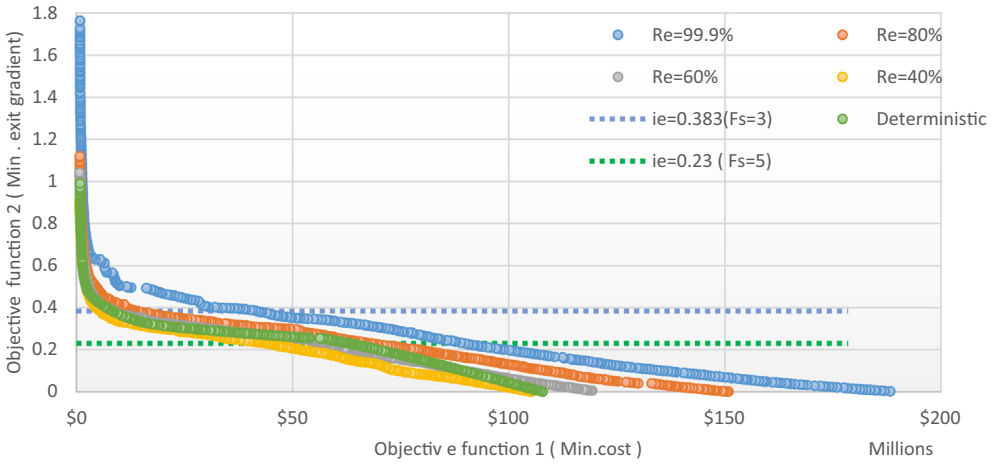

Fig. 15. Pareto front for different reliability levels (H = 60).

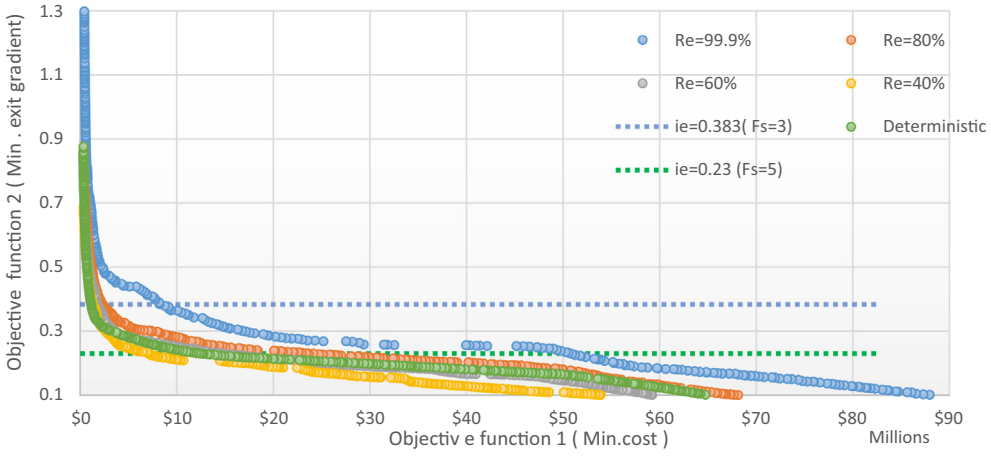

Fig. 16. Pareto front for different reliability levels (H = 40).

decision, the minimum allowable deterministic safe exit gradient values (Harr, 2012; Khosla et al., 1936) were used to locate the safe and feasible optimum solutions. In Figs. 13–17, the two horizontal lines show the locations of safety factors 5 and 3 for a critical gradient value of 1.15. Based on these values, the minimum safe exit gradient can be determined for the various reliability levels. To enhance the safety of the HWRS in terms of exit gradient, many possible non-dominated Pareto optimal solutions were available for consideration with ascending construction costs. An HWRS designer could use one of these solutions according to their preference.

The effects of reliability on the optimum HWRS designs for different head values were significant. Increasing reliability increased the construction cost. For instance, the minimum construction cost

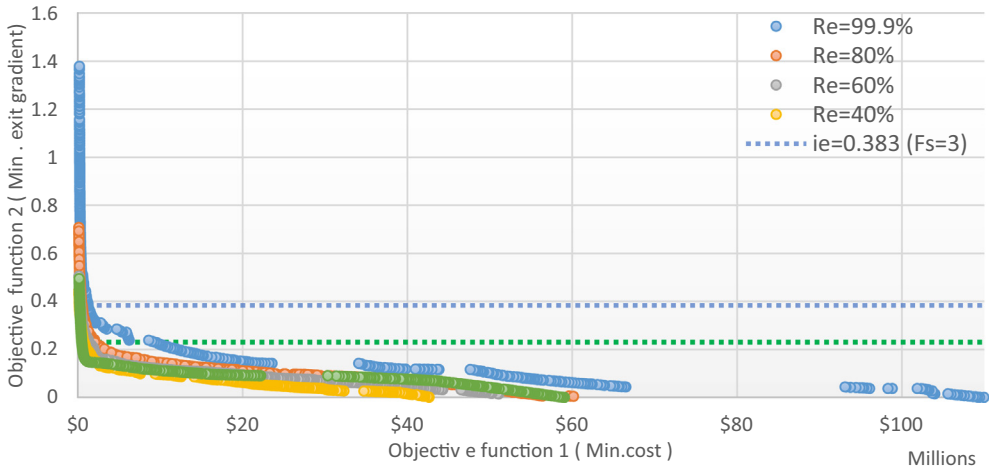

Fig. 17. Pareto front for different reliability levels (H = 20).

for H = 100 m, 40%, 60%, 80% and 100% reliability levels, and an exit gradient safety factor = 5 were $112,191,378.80, $129,171,757.66, $162,166,799.30 and $268,206,048.88, respectively. Similarly, the construction costs needed to satisfy an exit gradient = 3 were $59,951,442.01, $79,158,696.89, $106,049,766.41 and $160,838,745.00. This means that, in order to increase the reliability of the design from 60% to 100%, the construction cost would double. For high reliability levels, only a few feasible scenarios could be obtained from the Pareto optimal front. For example, for H = 100 m, 100% reliability and an exit gradient safety factor = 5, only a few points were found, at a higher construction cost of $268,206,048.88 (Fig. 13).

The deterministic optimum Pareto front related to the expected hydraulic conductivity (2 m/day) was also considered in this study. In general, the deterministic Pareto optimal front could be located close to a 60% reliability trade-off. However, some of the deterministic optimum solutions were less than the 40% reliability solutions. A 60% or 40% reliability means that there is an opportunity to find deterministic safety factors for an exit gradient value < 3, which might lead to piping failure. Based on this, we can deduce that the deterministic safety factors (3, 5) are insufficient to provide sufficient safety to such important HWRS projects, and they are inapplicable for measuring the safety of seepage designs that incorporate a certain degree of uncertainty. This is true if we assume that the prescribed safety factors are only used to quantify the uncertainty in the HHC.

Moreover, for all optimum solutions, the slope of the Pareto optimal front became smaller with small exit gradient values (<0.4). A significant cost was incurred in decreasing the exit gradient value by a small amount. Moreover, the most controllable design variable related to the exit gradient was d_2, which must be increased to reduce it. Besides, the equation that determines the cut-off construction cost is a function of d_2 (Eq. (17)). Consequently, when d_2 is increased, the construction cost increases substantially. Furthermore, because stochastic responses were included in the optimisation model, and the maximum value of many stochastic exit gradient values was minimised, the effects of reliability on construction cost were more pronounced when the exit gradient value (the second objective) was very small or approached zero (Figs. 13–17).

One advantage of using multi-objective optimisation in RBOD was the diversity of optimum solutions obtained. For (approximately) the same objective function values, the multi-objective optimisation model provided many optimum decision vectors (X). These solutions could not be obtained by formulating a single objective optimisation model. These solutions provide more flexible options because some optimum solutions are more applicable in terms of the design requirements, such as field limitations and construction procedures. Table 5 presents a few arbitrarily selected example solutions with the same objective function values including different optimum solution (X) scenarios.

The minimum and maximum feasible exit gradient optimum solutions for different reliability levels are listed in Tables 6–10. There were significant increases in construction cost for small decreases in exit gradient values. Also, it can be concluded from these results that d_2 plays a crucial role in reducing the exit gradient value.

Moreover, the main role of the first sheet pile depth d_1 is to reduce the uplift pressure under the foundation of the HWRS. However, d_1 also affects the exit gradient, because reducing the uplift pressure reduces the exit gradient. The optimum width, b, allows the design to satisfy the required overturning and sliding safety factors and prevent eccentric load conditions. These safety design requirements integrate b directly in their equations. The variable b^* is the part of the floor on the upstream side of the HWRS, which might be covered by water (Fig. 1). This variable is significantly associated with the safety and stability of an HWRS. The water covering b^* provides a cost-free source of weight on the HWRS that counterbalances the active momentums and forces that can weaken its stability. Some values of b^* approach the b value, which means that the majority of the HWRS floor is located on the upstream side. This also reflects the significance of this variable in terms of safety and minimising the cost of designs.

3.1. Evaluation of the methodology

Assessing the accuracy of the solutions is essential to validate the proposed methodology and demonstrate its potential applicability. Usually, to determine the accuracy of S-O model solutions obtained via a deterministic approach without considering uncertainties, the optimum solutions are input to the numerical simulation model, and the resulting seepage characteristics are compared with those predicted by the S-O model for the same optimum solution. The RBOD model, however, needs a different evaluation technique to quantify its accuracy, especially in terms of reliability. Furthermore, evaluation of the RBOD results does not include measurement of error for each seepage characteristic, as in deterministic evaluation.

Since quantifying the reliability of the optimum solution (design) is based on the multi-realisation technique, evaluation

Table 5
Different optimum solution values for same objective functions obtained by NSGA-II.

H	Reliability	Construction cost ($)	Exit gradient	d_1	d_2	b	b^*
20	40%	39,040,057.6	0.021	3.70	0.50	139.98	39.37
		38,711,633.0	0.021	0.78	3.06	30.93	15.17
40	40%	1,588,280.6	0.365	4.05	5.01	80.29	18.32
		1,544,093.7	0.366	4.16	21.37	46.74	40.80
60	40%	33,765,444.3	0.258	4.48	65.93	179.80	80.40
		33,427,294.7	0.261	61.72	54.47	78.96	49.82
80	40%	28,275,868.8	0.374	58.34	52.27	85.58	77.91
		27,327,404.2	0.374	30.73	65.07	75.37	74.53
20	99.9%	47,623,453.4	0.116	29.58	77.21	28.44	21.01
		43,815,973.8	0.117	45.77	72.83	21.15	19.56
60	99.9%	57,740,766.3	0.342	37.93	80.34	61.05	47.25
		56,752,425.9	0.343	71.71	62.54	86.34	46.50
20	80.0%	40,547,213.5	0.073	34.53	73.33	23.75	12.63
		40,367,765.1	0.074	72.09	41.34	39.87	29.61
80	60.0%	56,079,880.3	0.351	46.49	77.94	76.60	66.26
		55,187,390.3	0.351	26.17	80.08	76.11	68.53
40	60.0%	72,446,076.0	0.072	61.19	79.87	113.16	68.76
		66,394,331.9	0.072	47.71	82.12	68.76	59.16
100	40%	93,811,995.8	0.280	65.02	85.18	158.46	71.76
		93,403,373.0	0.282	56.51	88.54	92.46	91.59

Table 6
Minimum and maximum feasible solutions for different reliability levels (H = 100 m).

H	Reliability	Construction cost ($)	Exit gradient		d_1	d_2	b	b^*
100	100%	160,838,745.0	Max.Feasible	0.382	68.998	101.303	94.072	90.217
		291,913,182.3	Min.Feasible	0.211	98.277	110.000	92.960	86.702
	80%	106,049,766.4	Max.Feasible	0.383	64.37	89.62	97.56	96.01
		266,831,321.6	Min.Feasible	0.080	99.65	104.54	97.42	94.04
	60%	79,158,696.9	Max.Feasible	0.378	60.93	82.19	96.90	82.68
		253,417,538.3	Min.Feasible	0.022	95.21	105.57	113.05	83.98
	40%	59,951,442.0	Max.Feasible	0.381	51.30	78.04	93.07	92.66
		184,735,070.3	Min.Feasible	0.050	79.46	101.99	98.36	96.55
	Det.	88,783,399.4	Max.Feasible	0.381	53.53	87.91	92.23	88.42
		177,804,330.1	Min.Feasible	0.006	67.61	104.88	165.85	64.33

Table 7
Minimum and maximum feasible solutions for different reliability levels (H = 80 m).

H	Reliability	Construction cost ($)	Exit gradient		d_1	d_2	b	b^*
80	100%	102,526,240.8	Max.Feasible	0.382	55.04	91.69	77.43	77.24
		268,199,466.1	Min.Feasible	0.067	93.19	109.63	76.67	69.00
	80%	60,905,832.2	Max.Feasible	0.382	43.84	80.50	75.16	61.32
		208,554,042.6	Min.Feasible	0.016	90.48	100.37	79.83	61.35
	60%	38,552,199.4	Max.Feasible	0.382	57.18	63.58	76.63	69.80
		168,911,916.3	Min.Feasible	0.023	78.94	98.96	102.65	86.93
	40%	23,489,756.5	Max.Feasible	0.383	31.03	62.07	76.17	73.90
		135,258,887.1	Min.Feasible	0.039	68.42	95.94	103.61	66.13
	Det.	32,862,974.7	Max.Feasible	0.383	58.56	57.37	78.18	68.97
		139,701,276.7	Min.Feasible	0.0	57.32	100.20	82.90	49.22

Table 8
Minimum and maximum feasible solutions for different reliability levels (H = 60 m).

H	Reliability	Construction cost ($)	Exit gradient		d_1	d_2	b	b^*
60	100%	42,075,895.5	Max.Feasible	0.381	39.39	72.99	61.92	46.81
		188,247,133.9	Min.Feasible	0.002	79.94	102.64	67.92	36.71
	80%	14,352,204.0	Max.Feasible	0.383	33.28	52.83	64.91	52.24
		150,815,076.3	Min.Feasible	0.001	77.24	95.84	71.02	37.72
	60%	8,776,368.9	Max.Feasible	0.381	41.81	37.33	62.35	53.75
		119,297,688.9	Min.Feasible	0.005	65.41	93.24	70.85	47.82
	40%	5,634,374.6	Max.Feasible	0.382	29.68	37.36	77.08	53.21
		105,390,868.6	Min.Feasible	0.001	58.99	91.63	66.02	54.75
	Det.	8,474,313.2	Max.Feasible	0.382	27.84	45.39	58.24	49.15
		108,156,829.5	Min.Feasible	0.001	49.83	94.42	63.35	49.13

Table 9
Minimum and maximum feasible solutions for different reliability levels (H = 40 m).

H	Reliability	Construction cost ($)	Exit gradient		d_1	d_2	b	b*
40	100%	8,765,797.6	Max.Feasible	0.378	23.70	47.16	60.35	34.15
		151,144,025.4	Min.Feasible	0.001	86.85	89.16	63.35	25.76
	80%	2,406,236.8	Max.Feasible	0.380	22.71	29.43	44.61	36.62
		99,859,421.9	Min.Feasible	0.000	54.83	91.17	93.83	46.15
	60%	1,803,597.6	Max.Feasible	0.383	17.98	27.50	43.99	43.12
		80,204,409.8	Min.Feasible	0.043	64.50	81.31	110.50	64.33
	40%	1,334,875.1	Max.Feasible	0.380	21.88	21.01	48.75	31.61
		67,730,872.9	Min.Feasible	0.027	44.76	83.09	110.75	54.98
	Det.	1,171,848.0	Max.Feasible	0.383	14.15	22.77	52.09	36.74
		84,419,034.7	Min.Feasible	−0.001	37.01	89.64	62.92	53.37

Table 10
Minimum and maximum feasible solutions for different reliability levels (H = 20 m).

H	Reliability	Construction cost ($)	Exit gradient		d_1	d_2	b	b*
20	100%	1,262,284.3	Max.Feasible	0.380	19.86	23.99	27.68	25.03
		109,944,596.0	Min.Feasible	0.000	82.54	79.20	72.16	34.00
	80%	522,344.7	Max.Feasible	0.382	9.28	16.35	57.72	48.64
		60,149,842.6	Min.Feasible	0.004	39.48	81.20	115.27	95.03
	60%	338,708.5	Max.Feasible	0.383	8.88	14.60	30.27	22.13
		51,074,387.8	Min.Feasible	0.015	31.85	78.34	126.82	41.07
	40%	192,408.3	Max.Feasible	0.382	7.37	9.83	28.70	27.41
		42,940,043.9	Min.Feasible	0.000	40.37	73.39	138.01	42.74
	Det.	252,672.2	Max.Feasible	0.382	9.10	11.51	36.87	29.29
		92,965,180.5	Min.Feasible	−0.001	90.72	48.89	45.62	17.55

of the RBOD solutions is based on the number of realisations of the numerical simulations that satisfy the allowable limit of a specified safety factor to the total number of numerical runs incorporating different realisations of HHC. Hence, in this study, the evaluation method involved implementing the numerical seepage simulation for a selected optimum solution a specified number of times with different realisations of the HHC. The ratio of the number of times the allowable limit is satisfied to the total number of iterations provides a measure of the actual reliability level. Moreover, more accurate actual reliability levels could be estimated by implementing more iterations. In the present study, we simulated the seepage model using the implemented numerical simulation model code for the selected optimum solution set ten times for different realisations of the HHC to measure the actual reliability level.

Because the seepage design characteristic most impacted by uncertainty in HHC is the exit gradient at the four specified locations, these values were considered in order to evaluate the desired reliability level of the RBOD model. The other seepage quantities, such as the upstream and downstream uplift pressures, were less impacted by uncertainty in HHC.

The evaluation outcomes of four randomly selected optimum solutions demonstrate that the developed methodology provides reasonable indications of reliability, as shown in Tables 11–14. The exit gradient values in the tables were obtained from the numerical seepage simulations for the selected cases. The highlighted (in bold) exit gradient values were more than the safe allowable exit gradient value (0.382) obtained as a second objective function of the optimum solution. The desired reliability level, the objective function values, and the optimum solutions are shown in these tables. The CV for each implemented case was arbitrarily varied to evaluate the performance of the developed methodology with different CV values.

The average actual reliability (as verified by numerical simulation) in some cases, e.g. case A, was slightly less than the desired or specified reliability level (100%). In contrast, in other cases, such as case C, the average actual reliability level was greater than the desired reliability (60%). For other cases, the average actual reliability almost matched the desired levels, such as in cases B and D. Hence, the methodology developed to quantify the reliability of seepage predictions under various uncertainties provides an acceptable design solution with potential application to HWRS design problems in real-life cases. However, to ensure more accurate results, the number of iterations and the number of surrogate models incorporated in the RBOD must be increased.

Table 11
Evaluation results for case A (CV = 147.5%).

Case A	Rel. = 100%	Cost = 160838744$		ie = 0.382
Optimum design	***H*** ***100.0***	***d_1*** ***69.00***	***d_2*** ***101.3***	***b*** ***94.07***
Iteration	ie1	ie2	ie3	ie4
1	0.03	0.26	0.29	0.11
2	0.2	0.22	0.21	**0.67**
3	0.26	0.38	0.33	**0.45**
4	0.21	0.16	0.26	0.08
5	0.01	**0.42**	**0.48**	0.29
6	0.17	0.12	0.17	0.27
7	0.05	0.197	0.19	**1.28**
8	0.31	0.27	0.131	0.175
9	**0.56**	**0.41**	0.17	0.28
10	0.13	**0.58**	**0.54**	0.3
Actual reliability	90%	70%	80%	70%

Table 12
Evaluation results for case B (CV = 112.5%).

Case B	Rel. = 80%	Cost = 60905832		ie = 0.382
optimum design	***H***	***d_1***	***d_2***	***b***
	80.0	***43.84***	***80.5***	***75.16***
Iteration	ie_1	ie_2	ie_3	ie_4
1	**0.62**	0.44	0.18	0.2
2	0.16	0.24	0.26	0.22
3	0.09	**0.56**	**0.53**	0.132
4	**1.08**	**0.59**	0.08	**0.43**
5	0.33	0.198	0.2	0.21
6	0.17	0.24	0.19	**0.44**
7	0.7	0.38	0.15	0.15
8	0.17	**0.48**	0.37	0.25
9	0.12	0.24	**0.56**	**0.54**
10	0.25	0.32	0.37	0.23
Actual reliability	80%	70%	80%	70%

Table 13
Evaluation results for case C (CV = 182.5%).

Case C	Rel. = 60%	Cost = 1803597.62		ie = 0.383
optimum design	***H***	***d_1***	***d_2***	***b***
	40.00	***17.98***	***27.50***	***43.99***
Iteration	ie_1	ie_2	ie_3	ie_4
1	0.01	0.22	0.28	**0.98**
2	**0.49**	0.33	0.19	0.16
3	0.37	0.37	0.34	0.2
4	0.128	0.32	**0.63**	0.03
5	**0.53**	**0.52**	0.26	0.06
6	0.02	0.21	**0.42**	0.32
7	**0.54**	**0.45**	0.21	0.22
8	0.37	0.219	0.2	0.29
9	0.03	0.18	0.24	0.14
10	0.04	**0.95**	**0.96**	**0.61**
Actual reliability	70%	70%	70%	80%

Table 14
Evaluation results for case D (CV = 77.5%).

Case D	Rel. = 80%	Cost = 522344.7		ie = 0.382
Optimum design	***H***	***d_1***	***d_2***	***b***
	20.0	***9.28***	***16.3***	***57.72***
Iteration	ie_1	ie_2	ie_3	ie_4
1	0.34	0.28	0.17	0.29
2	0.1	0.09	**0.388**	**0.449**
3	0.14	0.36	**0.49**	0.33
4	**0.4**	0.31	0.17	**0.45**
5	0.146	0.168	0.24	**0.45**
6	**0.47**	0.27	0.1	**0.4**
7	0.06	0.15	0.26	0.2
8	0.08	0.15	0.2	0.34
9	0.31	0.19	0.2	0.29
10	0.22	0.16	0.27	**0.47**
Actual reliability	80%	100%	80%	60%

4. Conclusions

This study aimed to determine the safest HWRS designs at minimum construction cost by considering the uncertainty in seepage quantities due to uncertainty in HHC estimates. Although formulation of the RBOD based on the responses of a large number of surrogate models is a complex and time-consuming task, it was efficiently and successfully implemented based on a new formulation (MOMRO). Formulating RBOD problems as MOMRO models based on NSGA-II solver enhances the efficiency of population-based search processes to find the Pareto optimum solutions. In contrast to single optimisation techniques, the search process using the MOMRO technique was more efficient in approaching the global optimum solution. This formulation was based on the multi-realisation ‘‘staking” technique, which was used with the constraints and objective functions to incorporate reliability into the RBOD framework. This was achieved using 120 well-trained surrogate models based on the GPR technique to build six stochastic ensemble surrogate models that predict stochastic numerical seepage quantities (Pc_1, Pe_2, ie_1, ie_2, ie_3, ie_4).

Two strategies were adopted to drastically increase the RBOD computing efficiency. The first strategy involved the use of a nested function formulation and the second was the adaptation of the vector-process computing technique. These strategies improved

the computing efficiency of the MOMRO model by about 35 times compared to the conventional approach. This procedure also simplifies the selection process for NSGA-II parameters related to optimisation performance.

The proposed methodology was applied to hypothetical cases comprising four reliability levels (40%, 60%, 80%, 99.9%) and five upstream head values (100 m, 80 m, 60 m, 40 m, 20 m). The two objective functions minimised the exit gradient and construction costs. The results demonstrate that incorporating reliability into the optimisation model increases the safety of HWRS designs and strongly affects the optimum solutions. Ignoring uncertainty in hydraulic conductivity may negatively impact such designs. Increasing the specified reliability level significantly increases the construction cost due to increases in cut-offs depths and HWRS width.

High reliability levels (99.9% and 80%) made the optimum solutions for high upstream water head (100 m) infeasible with respect to exit gradient safety factors of five. The competing trade-off objectives encompassed numerous alternatives between the minimum exit gradient and minimum construction cost objective functions. The optimum solutions in the trade-off provided by the Pareto optimal solutions could aid HWRS designers in making more reliable and informed decisions. With some experience, additional reliability estimates and insight into rational optimum design could be achieved. Also, the safety factors inherent in the specified safe exit gradients can help select solutions at the optimum reliability levels. Furthermore, the MOMRO technique could provide, for the same objective functions values, many different optimum decision vectors (X). These results demonstrate the robustness of the MOMRO technique, which improves on the population-based search technique to attain the global optimum solution.

The evaluations show that the specified reliability levels agreed with the actual reliability levels. Also, the GPR-based surrogate models could predict the stochastic seepage quantities accurately and efficiently. However, there were some expected errors in the evaluation results. This could be attributed to the allowable error of the developed surrogate models and inadequate numbers of iterations being used to estimate the actual reliability level in the evaluation process.

Finally, historical records demonstrate that constructed HWRSs have a history of failure or unsatisfactory performance related to seepage in underlying porous media. The proposed methodology provides a promising procedure for obtaining optimal designs at minimum construction cost, and safe exit gradients with quantified design reliability. For future studies, to achieve greater reliability, it is recommended to incorporate other sources of uncertainty arising from surrogate model predictions, construction cost parameters, upstream water head fluctuations, and other related parameters. Also, the efficiency of utilised (deterministic) safety factors, which are considered in determining the optimum solutions, must be studied for various reliability levels.

Conflict of interest

The authors declared that there is no conflict of interest.

References

ACI Committee American Concrete Institute& International Organization for Standardization (2011). Building code requirements for structural concrete (ACI 318-11m) and commentary. Framington Hills, MI48331, USA: American Concrete Institute.

Ahmed, A. A. (2012). Stochastic analysis of seepage under hydraulic structures resting on anisotropic heterogeneous soils. *Journal of Geotechnical and Geoenvironmental Engineering, 139*(6), 1001–1004. https://doi.org/10.1061/%28ASCE%29GT.1943-5606.0000813.

Al-Juboori, M., & Datta, B. (2017a). Artificial neural network modeling and genetic algorithm based optimization of hydraulic design related to seepage under concrete gravity dams on permeable soils. Paper presented at the International Journal of Civil, Environmental, Structural, Construction and Architectural Engineering, Melbourne, Australia. http://waset.org/publications/10006237.

Al-Juboori, M., & Datta, B. (2017b). Influence of hydraulic conductivity and its anisotropy ratio on the optimum hydraulic design of water retaining structures founded on permeable soils. Paper presented at the 13th Hydraulics in Water Engineering Conference, Sydney, Australia.

Al-Juboori, M., & Datta, B. (2018b). Performance evaluation of a genetic algorithm-based linked simulation-optimization model for optimal hydraulic seepage-related design of concrete gravity dams. *Journal of Applied Water Engineering and Research, 1–25*. https://doi.org/10.1080/23249676.2018.1497558.

Al-Juboori, M., & Datta, B. (2018a). Linked simulation-optimization model for optimum hydraulic design of water retaining structures constructed on permeable soils. *International Journal of Geomate, 14*(44), 39–46. https://doi.org/10.21660/2018.44.7229.

Alpaydin, E. (2014). *Introduction to machine learning*. London, England: MIT Press.

Baecher, G. B., & Christian, J. T. (2005). *Reliability and statistics in geotechnical engineering*. West Sussex, England: John Wiley & Sons.

Baroni, G., Zink, M., Kumar, R., Samaniego, L., & Attinger, S. (2017). Effects of uncertainty in soil properties on simulated hydrological states and fluxes at different spatio-temporal scales. *Hydrology and Earth System Sciences, 21*(5), 2301. https://doi.org/10.5194/hess-21-2301-2017.

Bekele, E. G., & Nicklow, J. W. (2007). Multi-objective automatic calibration of SWAT using NSGA-II. *Journal of Hydrology, 341*(3–4), 165–176. https://doi.org/10.1016/j.jhydrol.2007.05.014.

Bligh, W. G. (1915). *Dams and weirs: An analytical and practical treatise on gravity dams and weirs; arch and buttress dams; submerged weirs; and barrages*. Chicago, USA: American Technical Society.

Burke, E. K., & Kendall, G. (2005). *Search methodologie*. Boston, USA: Springer.

Cho, S. E. (2012). Probabilistic analysis of seepage that considers the spatial variability of permeability for an embankment on soil foundation. *Engineering Geology, 133*, 30–39. https://doi.org/10.1016/j.enggeo.2012.02.013.

Christian, J. T., Ladd, C. C., & Baecher, G. B. (1994). Reliability applied to slope stability analysis. *Journal of Geotechnical Engineering, 120*(12), 2180–2207. https://doi.org/10.1061/(ASCE)0733-9410(1994) 120:12(2180).

Deb, K. (2001). *Multi-objective optimization using evolutionary algorithms* (Vol. 16) England: John Wiley & Sons.

Deng, Z.-P., Li, D.-Q., Qi, X.-H., Cao, Z.-J., & Phoon, K.-K. (2017). Reliability evaluation of slope considering geological uncertainty and inherent variability of soil parameters. *Computers and Geotechnics, 92*, 121–131. https://doi.org/10.1016/j.compgeo.2017.07.020.

Dhar, A., & Datta, B. (2009). Saltwater intrusion management of coastal aquifers. I: Linked simulation-optimization. *Journal of Hydrologic Engineering, 14*(12), 1263–1272. https://doi.org/10.1061/(ASCE)HE.1943-5584.0000097.

Dorsey, R., & Mayer, W. (1995). Genetic algorithms for estimation problems with multiple optima, nondifferentiability, and other irregular features. *Journal of Business & Economic Statistics, 13*(1), 53–66. https://doi.org/10.1080/07350015.1995.10524579.

Duncan, J. M. (2000). Factors of safety and reliability in geotechnical engineering. *Journal of Geotechnical and Geoenvironmental Engineering, 126*(4), 307–316. https://doi.org/10.1061/(ASCE)1090-0241(2000) 126:4(307).

European Committee For Standardization (2004). Eurocode 7: Geotechnical design-Part 1: General rules. British Standards. UK: CEN.

Freeze, R. A. (1975). A stochastic-conceptual analysis of one-dimensional groundwater flow in nonuniform homogeneous media. *Water Resources Research, 11*(5), 725–741. https://doi.org/10.1029/WR011i005p00725.

Gen, M., & Cheng, R. (2000). *Genetic algorithms and engineering optimization* (Vol. 7) USA: John Wiley & Sons.

Griffiths, D., & Fenton, G. A. (1993). Seepage beneath water retaining structures founded on spatially random soil. *Géotechnique, 43*(4), 577–587. https://doi.org/10.1680/geot.1993.43.4.577.

Griffiths, D., & Fenton, G. A. (1997). Three-dimensional seepage through spatially random soil. *Journal of Geotechnical and Geoenvironmental Engineering, 123*(2), 153–160. https://doi.org/10.1061/(ASCE)1090-0241(1997) 123:2(153).

Griffiths, D., & Fenton, G. A. (2004). Probabilistic slope stability analysis by finite elements. *Journal of Geotechnical and Geoenvironmental Engineering, 130*(5), 507–518. https://doi.org/10.1061/(ASCE)1090-0241(2004) 130:5(507).

Gupta, H. V., Sorooshian, S., & Yapo, P. O. (1999). Status of automatic calibration for hydrologic models: Comparison with multilevel expert calibration. *Journal of Hydrologic Engineering, 4*(2), 135–143. https://doi.org/10.1061/(ASCE)1084-0699(1999) 4:2(135).

Harr, M. E. (2012). *Groundwater and seepage*. New York, USA: McGraw Hill.

He, P., Li, S.-C., Xiao, J., Zhang, Q.-Q., Xu, F., & Zhang, J. (2017). Shallow sliding failure prediction model of expansive soil slope based on Gaussian process theory and its engineering application. *KSCE Journal of Civil Engineering, 22*(5), 1–11. https://doi.org/10.1007/s12205-017-1934-6.

Hicks, M. A., Nuttall, J. D., & Chen, J. (2014). Influence of heterogeneity on 3D slope reliability and failure consequence. *Computers and Geotechnics, 61*, 198–208. https://doi.org/10.1016/j.compgeo.2014.05.004.

Hicks, M. A., & Spencer, W. A. (2010). Influence of heterogeneity on the reliability and failure of a long 3D slope. *Computers and Geotechnics, 37*(7), 948–955. https://doi.org/10.1016/j.compgeo.2010.08.001.

Jiang, S.-H., Li, D.-Q., Zhang, L.-M., & Zhou, C.-B. (2014). Slope reliability analysis considering spatially variable shear strength parameters using a non-intrusive

stochastic finite element method. *Engineering Geology, 168*, 120–128. https://doi.org/10.1016/j.enggeo.2013.11.006.
Kang, F., Han, S., Salgado, R., & Li, J. (2015). System probabilistic stability analysis of soil slopes using Gaussian process regression with Latin hypercube sampling. *Computers and Geotechnics, 63*, 13–25. https://doi.org/10.1016/j.compgeo.2014.08.010.
Kang, F., Xu, B., Li, J., & Zhao, S. (2017). Slope stability evaluation using Gaussian processes with various covariance functions. *Applied Soft Computing, 60*, 387–396. https://doi.org/10.1016/j.asoc.2017.07.011.
Khosla, A. N., Bose, N. K., & Taylor, E. M. (1936). *Design of weirs on permeable foundations*. New Delhi: Central Board of Irrigation.
Kolda, T. G., Lewis, R. M., & Torczon, V. (2003). Optimization by direct search: New perspectives on some classical and modern methods. *SIAM Review, 45*(3), 385–482. https://doi.org/10.1137/S003614450242889.
Krahn, J. (2012). *Seepage modeling with SEEP/W: An engineering methodology*. Calgary, Alberta, Canada: GEO-SLOPE International Ltd..
Lambe, T. W., & Whitman, R. V. (2008). *Soil mechanics SI version*. New York: John Wiley & Sons.
Lane, E. W. (1935). Security from under-seepage-masonry dams on earth foundations. Paper presented at the Proceedings of ASCE.
Le, T. M. H., Gallipoli, D., Sanchez, M., & Wheeler, S. J. (2012). Stochastic analysis of unsaturated seepage through randomly heterogeneous earth embankments. *International Journal for Numerical and Analytical Methods in Geomechanics, 36*(8), 1056–1076. https://doi.org/10.1002/nag.1047.
Li, S.-C., He, P., Li, L.-P., Shi, S.-S., Zhang, Q.-Q., Zhang, J., & Hu, J. (2017). Gaussian process model of water inflow prediction in tunnel construction and its engineering applications. *Tunnelling and Underground Space Technology, 69*, 155–161. https://doi.org/10.1016/j.tust.2017.06.018.
Lj, T. (2014). *Dams and appurtenant hydraulic structures*. AA BALKEMA Pubi., Taylor & Francis Group pic.
Loyola, D., Pedergnana, M., & García, S. G. (2016). Smart sampling and incremental function learning for very large high dimensional data. *Neural Networks, 78*, 75–87. https://doi.org/10.1016/j.neunet.2015.09.001.
MathWorks (2015). Global optimization toolbox user's guide R2015b. www.mathworks.com.
Mollon, G., Dias, D., & Soubra, A.-H. (2009). Probabilistic analysis of circular tunnels in homogeneous soil using response surface methodology. *Journal of Geotechnical and Geoenvironmental Engineering, 135*(9), 1314–1325. https://doi.org/10.1061/(ASCE)GT.1943-5606.0000060.
Mollon, G., Dias, D., & Soubra, A.-H. (2010). Probabilistic analysis of pressurized tunnels against face stability using collocation-based stochastic response surface method. *Journal of Geotechnical and Geoenvironmental Engineering, 137*(4), 385–397. https://doi.org/10.1061/(ASCE)GT.1943-5606.0000443.
Moriasi, D. N., Arnold, J. G., Van Liew, M. W., Bingner, R. L., Harmel, R. D., & Veith, T. L. (2007). Model evaluation guidelines for systematic quantification of accuracy in watershed simulations. *Transactions of the ASABE, 50*(3), 885–900. https://doi.org/10.13031/2013.23153.
Pal, M., & Deswal, S. (2010). Modelling pile capacity using Gaussian process regression. *Computers and Geotechnics, 37*(7–8), 942–947. https://doi.org/10.1016/j.compgeo.2010.07.012.
Popescu, R., Deodatis, G., & Nobahar, A. (2005). Effects of random heterogeneity of soil properties on bearing capacity. *Probabilistic Engineering Mechanics, 20*(4), 324–341. https://doi.org/10.1016/j.probengmech.2005.06.003.
Rajabi-Bahaabadi, M., Shariat-Mohaymany, A., Babaei, M., & Ahn, C. W. (2015). Multi-objective path finding in stochastic time-dependent road networks using non-dominated sorting genetic algorithm. *Expert Systems with Applications, 42*(12), 5056–5064. https://doi.org/10.1016/j.eswa.2015.02.046.
Rasmussen, C. E. (2004). Gaussian processes in machine learning. In *Advanced lectures on machine learning* (pp. 63–71). Berlin, Heidelberg: Springer.
Roberts, S., Osborne, M., Ebden, M., Reece, S., Gibson, N., & Aigrain, S. (2013). Gaussian processes for time-series modelling. *Philosophical Transactions of the Royal Society A, 371*, 20110550. https://doi.org/10.1098/rsta.2011.0550.
Ross, S. (2014). *A first course in probability*. Boston, MA, USA: Pearson.
Samui, P., & Jagan, J. (2013). Determination of effective stress parameter of unsaturated soils: A Gaussian process regression approach. *Frontiers of Structural and Civil Engineering, 7*(2), 133–136. https://doi.org/10.1007/s11709-013-0202-1.
Shahrbanozadeh, M., Barani, G.-A., & Shojaee, S. (2015). Simulation of flow through dam foundation by isogeometric method. *Engineering Science and Technology, an International Journal, 18*(2), 185–193. https://doi.org/10.1016/j.jestch.2014.11.001.
U.S. Army Corps of Engineers (1987) Engineering and design flotation stability criteria for concrete hydraulic structures. http://www.dtic.mil/dtic/tr/fulltext/u2/a403467.pdf.
Yandamuri, S., Srinivasan, K., & Murty Bhallamudi, S. (2006). Multiobjective optimal waste load allocation models for rivers using nondominated sorting genetic algorithm-II. *Journal of Water Resources Planning and Management, 132*(3), 133–143. https://doi.org/10.1061/(ASCE)0733-9496(2006) 132:3(133).
Yapo, P. O., Gupta, H. V., & Sorooshian, S. (1998). Multi-objective global optimization for hydrologic models. *Journal of Hydrology, 204*(1–4), 83–97. https://doi.org/10.1016/S0022-1694(97)00107-8.
Zakaria, M. Z., Jamaluddin, H., Ahmad, R., & Loghmanian, S. M. (2012). Comparison between multi-objective and single-objective optimization for the modeling of dynamic systems. *Journal of Systems and Control Engineering, 226*(7), 994–1005. https://doi.org/10.1177/0959651812439969.
Zhu, X., Wang, X., Li, X., Liu, M., & Cheng, Z. (2017). A new dam reliability analysis considering fluid structure interaction. *Rock Mechanics and Rock Engineering, 1–12*. https://doi.org/10.1007/s00603-017-1369-x.